

**COLLISION-INDUCED 1st OVERTONE INFRARED ABSORPTION
BAND OF DEUTERIUM**

CENTRE FOR NEWFOUNDLAND STUDIES

**TOTAL OF 10 PAGES ONLY
MAY BE XEROXED**

(Without Author's Permission)

CHING-ZHY KUO, B.Sc



COLLISION-INDUCED 1ST OVERTONE INFRARED ABSORPTION
BAND OF DEUTERIUM

by

Ching-Zhy Kuo, B.Sc.

Submitted in partial fulfilment
of the requirements for the degree of Master of Science
Memorial University of Newfoundland

April, 1970

CONTENTS

ABSTRACT

(iii)

CHAPTER 1.	INTRODUCTION	1
1.1	Collision-Induced Absorption of the Infrared Fundamental Bands of Hydrogen and Deuterium	1
1.2	Collision-Induced 1st Overtone Infrared Absorption Band of Hydrogen	3
1.3	A Brief Outline of the Theory of Collision- Induced Absorption in the Fundamental and 1st Overtone Bands of Symmetric Diatomic Gases	4
1.4	Collision-Induced 1st Overtone Infrared Absorption Band of Deuterium	6
CHAPTER 2.	EXPERIMENTAL TECHNIQUE	9
2.1	Construction Details of the 2m Absorption Cell	9
2.2	Optical Arrangement	13
2.3	Experimental Procedure	15
2.4	Reduction of Experimental Traces	18
2.5	Isothermal Data of Gases	20
2.6	A Note on the Errors of Observation	21
CHAPTER 3.	EXPERIMENTAL RESULTS AND DISCUSSION	24
3.1	Absorption Profiles of the 1st Overtone Band of Deuterium in D ₂ -Ar, D ₂ -N ₂ and Pure D ₂	24
3.2	Absorption Coefficients of the 1st Overtone Band of Deuterium	33

CHAPTER 4. ANALYSIS OF THE ENHANCEMENT ABSORPTION PROFILES	47
4.1 Introduction	47
4.2 The Quadrupole-Induced 1st Overtone Band	48
4.3 Relative Intensities of the Quadrupolar Single-Transition Components	51
4.4 Line Shape	52
4.5 Analysis of the Profiles of the 1st Overtone Band in D ₂ -Ar and D ₂ -N ₂ Mixtures	54
4.6 Discussion	57
APPENDIX A. THE THEORY OF COLLISION-INDUCED INFRARED ABSORPTION	63
APPENDIX B MATRIX ELEMENTS OF THE QUADRUPOLE MOMENT FOR THE TRANSITIONS IN THE 1ST OVERTONE BAND OF DEUTERIUM	73
APPENDIX C. NORMALIZED BOLTZMANN FACTORS OF THE ROTATIONAL LEVELS OF THE GROUND VIBRATIONAL STATE OF D ₂	78
APPENDIX D. RACAH COEFFICIENTS OF DIFFERENT BRANCHES IN THE INDUCED VIBRATION-ROTATION SPECTRA	81
ACKNOWLEDGMENTS	84
REFERENCES	85

ABSTRACT

The collision-induced 1st overtone infrared absorption band of deuterium was observed at room temperature. The band was studied in the pure gas and in binary mixtures with argon and nitrogen at a path length of 194.3 cm at pressures up to 800 atm. The observed absorption profiles of the band do not show any splitting of the Q branch and this indicates that the contribution of the short-range overlap forces to the intensity of the band is negligible. The enhancement absorption profiles of D_2 -Ar mixtures show only single-transition quadrupolar lines. But the enhancement profiles of D_2 - N_2 mixtures, in addition, show the double transitions $Q_2(J)$ of D_2 + $S_0(J)$ of N_2 , and double vibrational transitions $Q_1(J)$ of D_2 + $Q_1(J)$ of N_2 which occur on the low frequency side of the pure overtone band. Major contribution to the intensity of the absorption profiles of pure deuterium comes from the double transitions $Q_2(J) + S_0(J)$ and $Q_1(J) + Q_1(J)$ in the colliding pairs of D_2 molecules. Integrated absorption coefficients were measured and binary and ternary absorption coefficients were derived.

The observed enhancement absorption profiles of D_2 -Ar and D_2 - N_2 were analyzed by a computational procedure into their component lines to yield values of the half widths δ_s . The analysis of the profiles of D_2 -Ar confirmed the fact that the contribution of the overlap forces to the intensity of the band is negligible. From the analysis of the pure overtone profiles of D_2 - N_2 , the contribution of the double transitions, $Q_2(J)$ of D_2 + $S_0(J)$ of N_2 , to the intensity of the band was estimated. The quadrupole moment of the nitrogen molecule was obtained

(iv)

as 1.14 ea_0^2 from the ratio of the binary absorption coefficients of the band due to single and double transitions.

CHAPTER 1

INTRODUCTION

1.1 Collision-Induced Absorption of the Infrared Fundamental Bands of Hydrogen and Deuterium

The collision-induced fundamental infrared absorption band of gaseous hydrogen first observed by Welsh, Crawford and Locke (1949) has been extensively studied in the pure gas and in binary mixtures with foreign gases over a variety of experimental conditions (for references, see Varghese and Reddy, 1969). A detailed investigation of the collision-induced fundamental band of gaseous deuterium has been made at room temperature by Reddy and Cho (1965) in the pure gas at pressures up to 250 atm and Pai, Reddy and Cho (1966) in D_2 -He, D_2 -Ar and D_2 - N_2 mixtures at pressures up to 1200 atm. The band has been investigated by Watanabe and Welsh (1965) in the pure gas at low pressures in the temperature range 24^0K to 77^0K . Sinha (1967) made some preliminary studies of the band in the pure gas and D_2 -He and D_2 -Ne mixtures at low temperatures. Russell (1968) made a systematic study of the band in D_2 -He and D_2 -Ne mixtures at different temperatures in the range 77^0K to 298^0K . In most of these studies, it was observed that the integrated absorption coefficient of the induced fundamental band in the pure gas and the enhancement in the integrated absorption coefficient of the band in the mixtures are density-dependent. For the pure gas the integrated absorption coefficient is given approximately by

$$\int \alpha(v) dv = \alpha_{1a}^2 a^2 + \alpha_{2a}^3 a^3$$

and for the mixtures the enhancement in the integrated absorption coefficient is given approximately by

$$\int \alpha_{en}(v) dv = \alpha_{1b}^2 a^2 b^2 + \alpha_{2b}^3 a^3 b^3 .$$

Here the subscripts a and b refer to the absorbing and perturbing gases respectively, α_{1a} and α_{1b} are binary absorption coefficients resulting from binary collisions of types a-a and a-b respectively, and α_{2a} and α_{2b} are ternary absorption coefficients resulting from ternary collisions of types a-a-a and b-a-b respectively.

The induced fundamental bands of hydrogen and deuterium consist of three types of transitions: $Q_1(J)$ transitions ($\Delta v = 1, \Delta J = 0$), $S_1(J)$ transitions ($\Delta v = 1, \Delta J = +2$) and $O_1(J)$ transitions ($\Delta v = 1, \Delta J = -2$). Since the forbidden transitions in the infrared absorption of symmetric diatomic gases occur as a result of an induction mechanism, it is to be expected that these transitions obey the rotational selection rules similar to those in Raman spectra. The Q_1 branch of these fundamental bands has a minimum in the neighborhood of the band origin and two broad components Q_P and Q_R at lower and higher frequency respectively. The separation between the maxima of these components Δv_{PR}^{max} increases with the density of the mixture. The Q_1 branch consists of overlap and quadrupolar components denoted as $Q_{overlap}(J)$ and $Q_{quad}(J)$ respectively. According to the theory of Van Kranendonk (1958), the $Q_{overlap}(J)$ components arise due to the short-range electron overlap forces while

$Q_{\text{quad}}(J)$, $S(J)$ and $O(J)$ components occur as a result of the long-range quadrupolar induction. In collision-induced spectra, the overlap as well as the quadrupolar components are modulated by the translational motion of the colliding molecules. The frequency distribution of each component is represented as the summation and difference tones $\nu_m(J) \pm \nu_{tr}$ where $\nu_m(J)$ is the molecular frequency of the transition and ν_{tr} is the continuum of frequencies for all possible values of the relative translational energy of the colliding pair of molecules. It is known both experimentally and theoretically that in the induced fundamental band, if the perturbing molecule has no quadrupole moment, only single transitions occur in the spectra and if it has a quadrupole moment, single as well as double transitions occur (see Chapters 3 and 4).

1.2 Collision-Induced 1st Overtone Infrared Absorption Band of Hydrogen

The quadrupolar first and second overtone infrared absorption bands of hydrogen were first observed by Herzberg (1950). The collision-induced 1st overtone infrared absorption band of hydrogen was first observed by Welsh, Crawford, MacDonald and Chisholm (1951) and later studied by Hare and Welsh (1958) at room temperature, Hunt (1959) at 85°K , 195°K and 300°K , and Watanabe (1964) at 24°K . This collision-induced 1st overtone band has been interpreted as a superposition of two profiles. One of these profiles is a pure overtone band in which the transition $\Delta\nu = 2$ takes place in one of the colliding molecules, and the other corresponds to a double vibrational transition in which each molecule of the pair performs the fundamental vibrational transition. In

these studies, the Q lines of the 1st overtone band show no indication of splitting or broadening even at a pressure of 500 atm (Hare and Welsh, 1958). In the studies at low temperatures (Hunt, 1959 and Watanabe, 1964), single transitions $Q_2(1)$, $S_2(0)$, $S_2(1)$ and double vibrational transitions of the type $Q_1(J) + Q_1(J)$ and double transitions of the type $Q_2(J) + S_0(J)$ have been observed (the reader is referred to section 4.2 for a discussion of single and double transitions in the 1st overtone band).

1.3 A Brief Outline of the Theory of Collision-Induced Absorption in the Fundamental and 1st Overtone Bands of Symmetric Diatomic Gases

A detailed summary of the theory of collision-induced infrared absorption of the fundamental and 1st overtone bands is given in Appendix A. Collision-induced infrared fundamental absorption band of a symmetric diatomic gas was theoretically treated by Van Kranendonk (1957, 1958) who proposed the so-called "exp-4" model for the induced dipole moment in a binary collision between a symmetric diatomic molecule and a perturbing molecule. In this model, the induced dipole moment consists of two additive parts. One of these is the angle-independent (isotropic) short-range electron overlap moment which decreases exponentially with the intermolecular distance R and mainly contributes to the intensity of the Q branch. The other part is the angle-dependent (anisotropic) long-range dipole moment resulting from the polarization of one molecule by the quadrupole field of the other and is proportional to R^{-4} . This part contributes to the intensity of the O, Q and S branches. The quadrupole contribution to the Q branch is referred to as the Q_{quad} component.

When the exp-4 model and the Lennard-Jones potential are used for the induced dipole moment and the intermolecular potential respectively, the binary absorption coefficient due to collisions between molecules 1 and 2 can be written as (see Appendix A)

$$\tilde{\alpha}_{1a} \text{ or } \tilde{\alpha}_{1b} = \lambda^2 \mathbf{I} \tilde{\gamma} + \left\{ \left(\frac{Q_1 \alpha_2}{e\sigma} \right)^2 + \left(\frac{\alpha_1 Q_2}{e\sigma} \right)^2 \right\} \mathbf{J} \tilde{\gamma} ,$$

where $\lambda^2 \mathbf{I} \tilde{\gamma}$ is the overlap part of the binary absorption coefficient and the remaining terms on the right-hand side of the equation represent the quadrupolar part. Here λ is the overlap parameter, characteristic of the overlap part of the induced dipole moment, $\tilde{\gamma}$ is a constant, Q is the quadrupole moment, α is the polarizability, single prime represents the first derivative with respect to internuclear distance, \mathbf{I} and \mathbf{J} are dimensionless definite integrals which depend respectively on the range ρ of the overlap moment and the pair distribution function g , e is the electronic charge and σ is the Lennard-Jones diameter of the colliding pair of molecules.

The experimental profiles of the 1st overtone band of hydrogen obtained by earlier researchers and those of the 1st overtone band of deuterium obtained in the present work indicate that the overlap contribution to the intensity of the band is negligible. Therefore, the binary absorption coefficient corresponding to the pure overtone profile of the 1st overtone band can be represented by (also see Appendix A)

$$\tilde{\alpha}_{1a} \text{ or } \tilde{\alpha}_{1b} = \frac{k_1^2}{2} \left\{ \left(\frac{Q_1 \alpha_2}{e\sigma} \right)^2 + \left(\frac{\alpha_1 Q_2}{e\sigma} \right)^2 \right\} \mathbf{J} \tilde{\gamma}$$

where k_1 is a constant and double prime represents the second derivative* with respect to the internuclear distance.

The binary absorption coefficient corresponding to the profile due to double vibrational transitions of the 1st overtone band can be written as (also see Appendix A)

$$\tilde{\alpha}_1^{\text{d.v.}} = k_1^2 \left\{ \left(\frac{Q_1 \alpha_2}{e\sigma^4} \right)^2 + \left(\frac{\alpha_1 Q_2}{e\sigma^4} \right)^2 \right\} J \bar{\gamma} .$$

1.4 Collision-Induced 1st Overtone Infrared Absorption Band of Deuterium

Prior to the work presented in this thesis, no work has been reported on the collision-induced 1st overtone band of deuterium. To illustrate possible single transitions between the lower and upper rotational states of the 1st overtone absorption band of deuterium (i.e. $v' = 2, J' \leftarrow v'' = 0, J''$), a schematic energy level diagram is presented in Fig. 1. Here the vibrational and rotational term values $G_0(v)$ and $F_v(J)$, respectively, were calculated from the constants of the free molecule (Stoicheff, 1957 and Wilkinson, 1968). However, if the perturbing molecule has a quadrupole moment, several double transitions will contribute to the intensity of the band, but these were not shown in Fig. 1. The relative population of the deuterium molecules in various rotational states at a given temperature depends on the Boltzmann distribution law, the $(2J + 1)$ -fold degeneracy and the degeneracy due to nuclear spin.

In the present investigation, the collision-induced 1st overtone absorption band of deuterium has been observed in the pure gas

*With harmonic oscillator approximation.

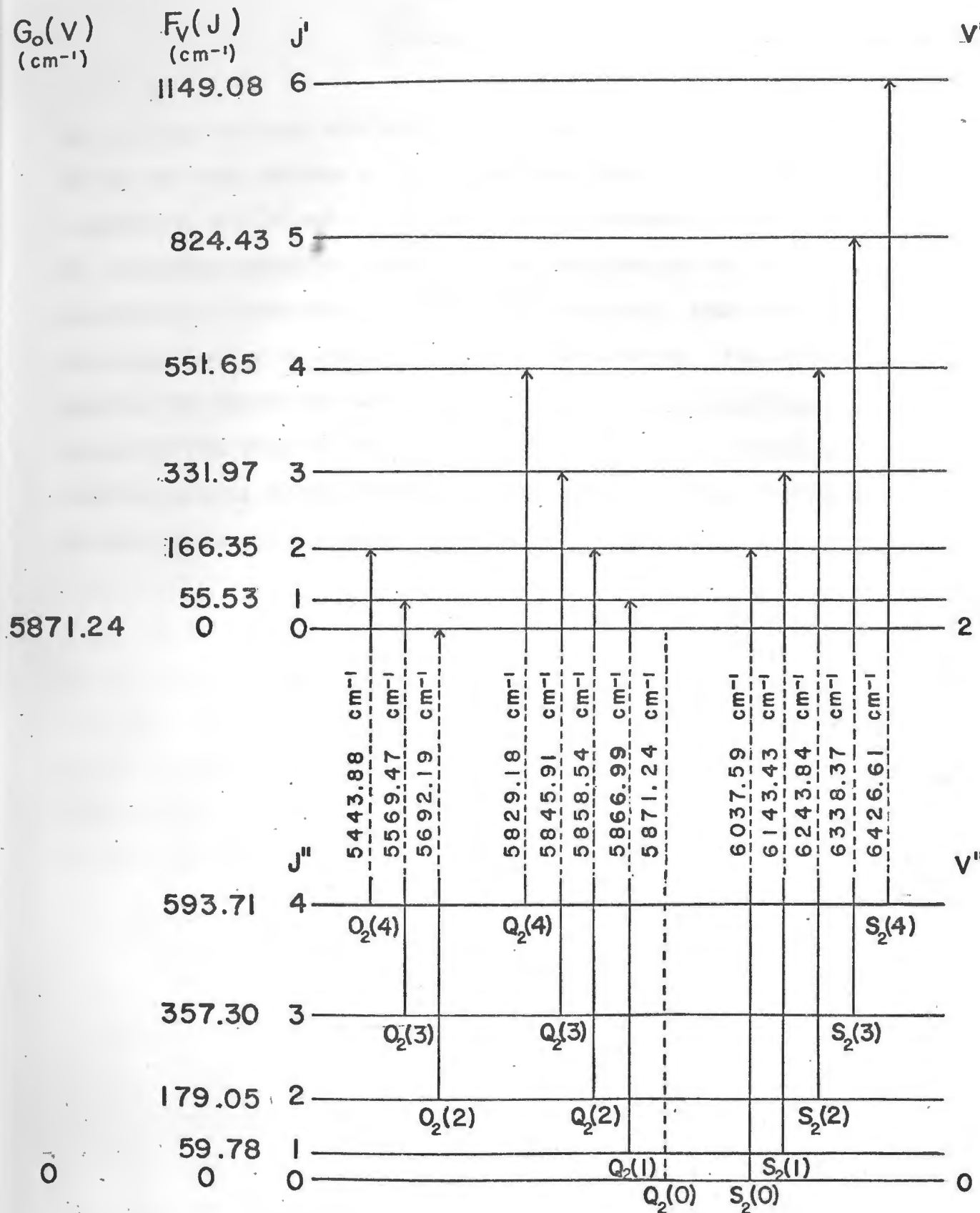


Fig. 1. Single transitions in the induced 1st overtone band of deuterium.

and in binary mixtures with argon and nitrogen. The absorption profiles of the band were obtained at room temperature using a high pressure transmission cell of path length 194.3 cm and pressures up to 800 atm. The integrated absorption coefficients for the pure gas and the enhancements of these for the mixtures were measured. From these, the binary and ternary absorption coefficients were derived. The profiles obtained for the mixtures were analyzed using a Boltzmann-modified dispersion line shape for the individual single transition components. From the analysis of the profiles of D₂-N₂ mixtures, it was possible to estimate the quadrupole moment of nitrogen.

CHAPTER 2

EXPERIMENTAL TECHNIQUE

The object of the present work was to obtain reasonably accurate values of the binary and ternary absorption coefficients of the collision-induced first overtone band of deuterium. An absorption cell of long path was required in order to keep the working pressure in the experiments at moderate values. A high pressure cell of length 2m designed recently for this type of work was used to study the absorption in the pure deuterium gas and in D₂-N₂ and D₂-Ar mixtures at room temperature. The maximum pressure reached in the experiments was 12,000 p.s.i. The first overtone band of deuterium lies in the infrared spectral region 5100 cm⁻¹ - 6600 cm⁻¹. A Perkin-Elmer Model 112 single-beam double-pass spectrometer with LiF prism and a Kodak Ektron PbS cell of type N was used to record the spectra. The details of the design and construction of the absorption cell and of the experimental procedure used in the present investigation form the rest of this chapter.

2.1 Construction Details of the 2m Absorption Cell

The details of the construction of the 2m transmission-type absorption cell are shown in Figs. 2 and 3. The body of the cell and most of its accessories were made of type-303 stainless steel. The body of the cell H is 2m long, 1 in. in wall thickness and 3 in. in outside diameter. The central bore of 1 in. with an accuracy of $\pm .010$ in. in the body of the cell was drilled by Industrial Machining Limited, Montreal, Quebec. A light guide G with a rectangular aperture of

1 cm x .5 cm, made in five pieces, was inserted into the central bore of the cell. The inner surface of the light guide was polished so that reflection, and hence transmission of radiation would be good. The entrance and exit windows, W, were polished synthetic sapphire plates, 1 cm in thickness and 1 in. in diameter. These windows were cemented onto the window plates, P, with General Electric glyptal. Steel caps, C, with teflon washers, T, placed in between the steel caps and the windows to prevent chipping, held the windows in position during evacuation of the cell. The apertures in the window plates were of the same dimensions as the aperture of the light guide. The apertures of the assembled cell were designed to allow a f/4 cone of radiation from the source and the spectrometer slit to focus onto the entrance and exit ends of the cell respectively. Each window plate was provided with a side pin which fitted exactly into a matched pin recess in the cell body (not shown in Fig. 2). This arrangement prevented non-alignment of the apertures in the window plates with that of the light guide. A good pressure seal was obtained by using deoxydized copper O-rings, O, .075 in. thick (Fig. 3), between the window plates and the cell body. Each of the end pieces, N, 1.65 in. thick and 3.5 in. in diameter are flat plates having a central conical bore of 15° (Fig. 3). These end pieces were tightened against the cell body with the help of eight Allenoy steel Allen socket-head cap screws, S, each 3/8 in. in diameter. A 1/4 in. diameter steel capillary tube, A, served as the gas inlet to the cell and was connected by means of an Aminco-fitting (Fig. 2). When the cell is assembled, its effective path length (from one window surface to the other) is 194.3 cm at room temperature.

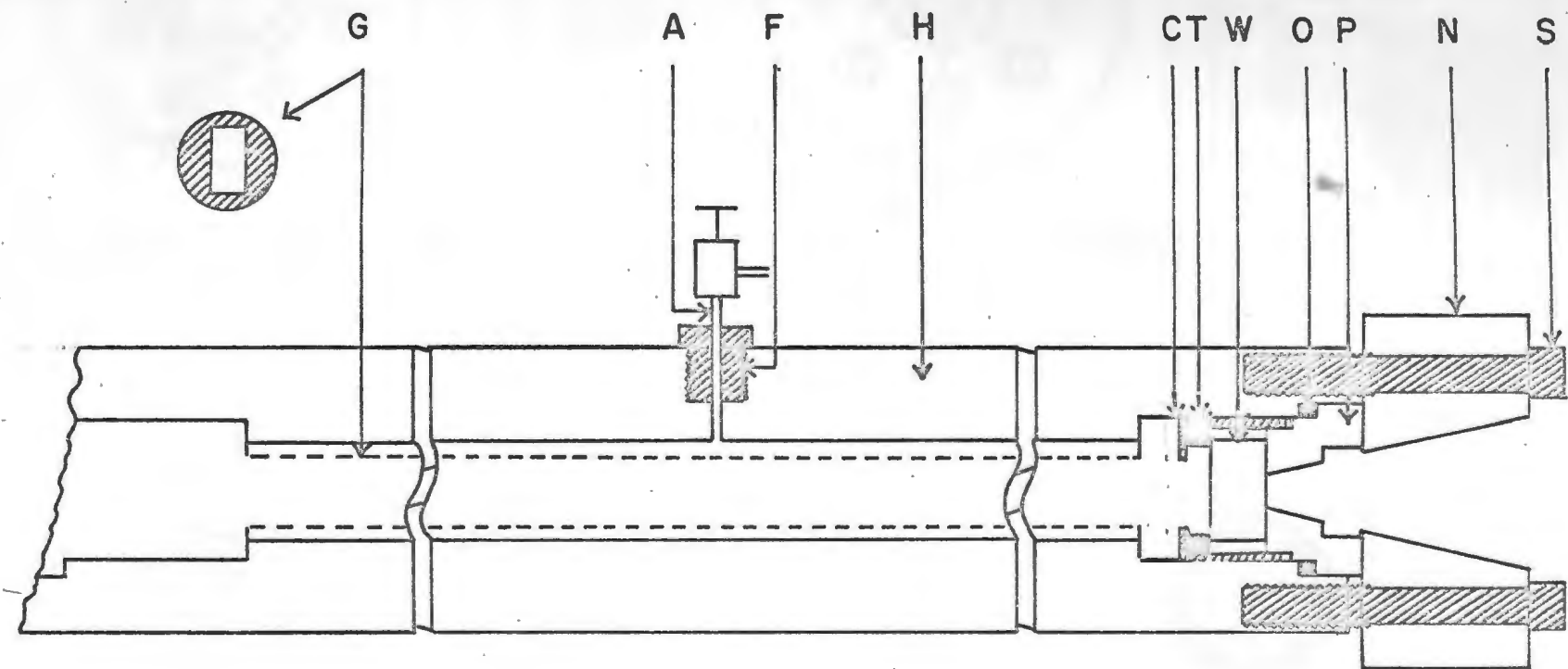
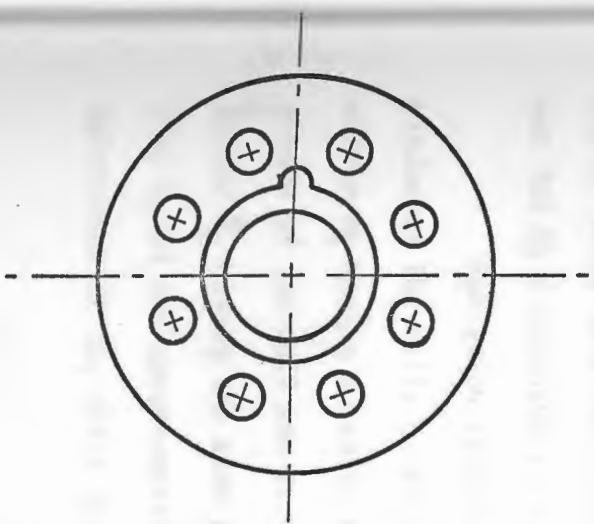
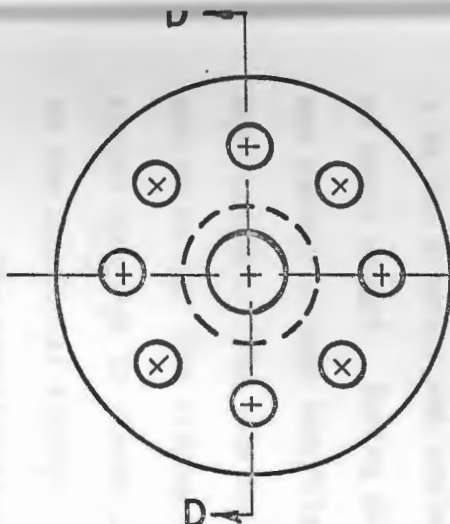


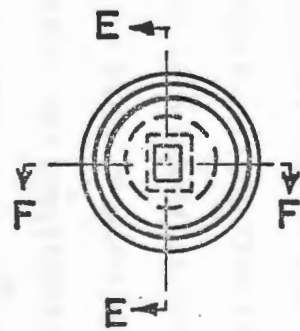
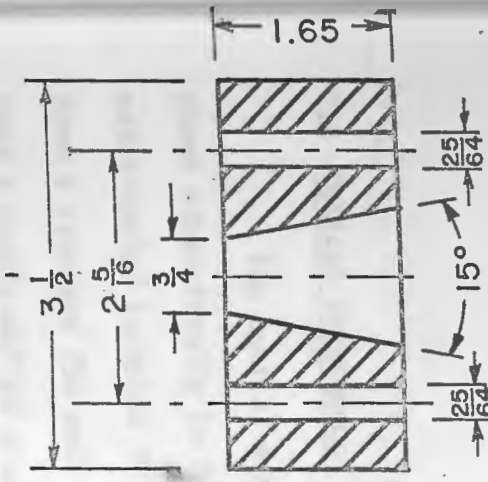
Fig. 2. A cross section of the 2m high pressure absorption cell.



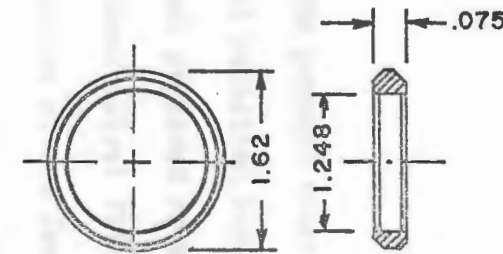
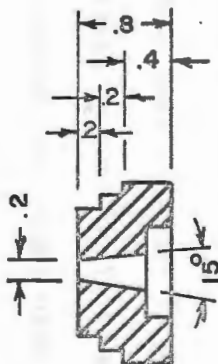
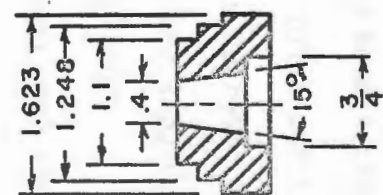
(a) END VIEW OF CELL BODY



(b) END PIECE



(c) WINDOW PLATE



(d) COPPER O-RING

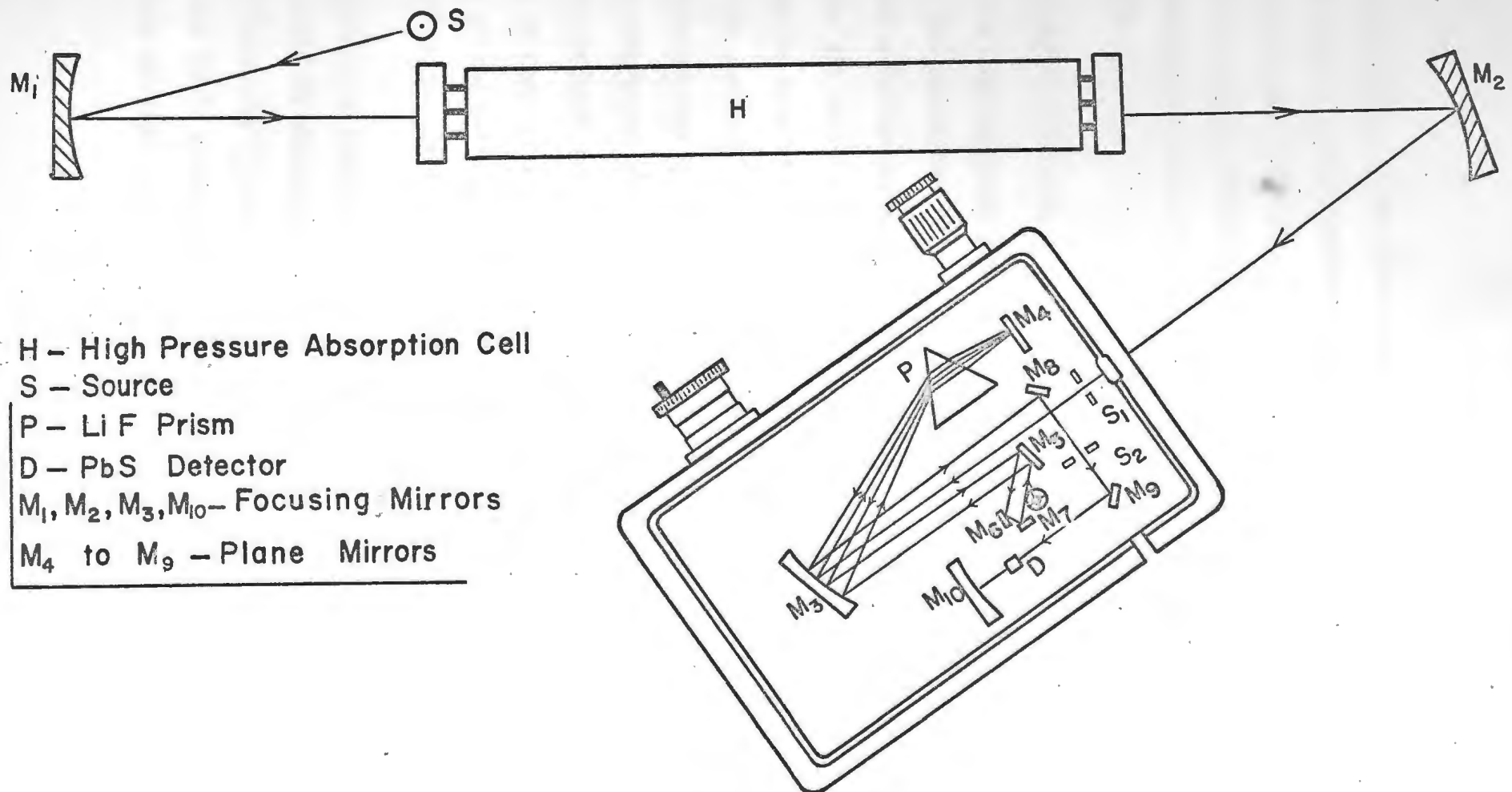
Fig. 3. Accessories of 2m absorption cell: (a) End view of the cell body (b) End piece (c) Window plate (d) Copper O-ring. (All the lengths are in inches.)

2.2 Optical Arrangement

The optical arrangement used in the present investigation is shown schematically in Fig. 4. The infrared radiation source, S, was a water-cooled tungsten filament lamp which was prepared in our laboratory from a standard 750 watt projection bulb planar spiral filament sealed into a double-walled glass envelope. A sapphire window 2mm thick and 1 in. in diameter was sealed onto the opening in this envelope by means of Hysol cement. During the evacuation of the lamp, a small current was passed through the filament to remove impurities that might have been present. The lamp was filled with pure nitrogen to a pressure of 600 mm of Hg. The nitrogen was purified by passing it slowly over hot copper turnings to remove traces of oxygen that might have been present in the commercial supply.

The experiments were performed with a Perkin-Elmer Model 112 single-beam double-pass spectrometer using LiF prism and a PbS detector operated at room temperature. The source S was operated at 4.2 amps and 50 volts obtained from a stabilized a.c. power supply unit which was fed by a Sorenson a.c. regulator, Model ACR-2000.

Radiation from the source S was focused onto the entrance window of the cell, H, by an aluminized spherical concave front surface mirror M_1 having a radius of curvature of 42 cm. Light from the exit window of the cell was reflected and focused by a spherical concave mirror M_2 having the same radius of curvature as M_1 onto the entrance slit S_1 of the spectrometer. The slit width of the spectrometer was maintained at 50μ which gave a spectral resolution of 11 cm^{-1} at



H – High Pressure Absorption Cell

S – Source

P – Li F Prism

D – PbS Detector

M_1, M_2, M_3, M_{10} – Focusing Mirrors

M_4 to M_9 – Plane Mirrors

Fig. 4. A schematic diagram of the optical arrangement.

5871 cm^{-1} , the origin of the first overtone band of deuterium. Light cones of f/4 were used throughout the optical arrangement. The spectral region from 5100 cm^{-1} to 6600 cm^{-1} was calibrated using the known frequencies of mercury emission lines (Humphreys, 1953) and absorption peaks of polystyrene and 1,2,4,-trichlorobenzene (Plyler, Blaine, and Nowak, 1957).

2.3 Experimental Procedure

The high pressure gas handling system used to introduce the gases into the absorption cell, H, is shown schematically in Fig. 5. Prior to the actual experiments, the absorption cell and the appropriate parts of the gas handling system were tested for high pressures and for good vacuum for several days. In Fig. 5, G_1 and G_2 are Bourdon pressure gauges in the ranges 0 - 5000 p.s.i. and 0 - 20,000 p.s.i. respectively, which were calibrated by an Ashcroft dead weight tester, C is a mercury-column gas compressor operated by an Aminco oil pump, V_1 to V_7 are Aminco high pressure valves, and T_1 and T_2 are liquid nitrogen/oxygen traps made of copper tubing, 1/4 in. in outside diameter. Different components of the system were connected by stainless steel capillary tubing, 1/4 in. in outside diameter.

Pure Deuterium Experiments:

With the absorption cell evacuated, recorder traces of the background intensity I_0 were taken until they were reproducible. Then deuterium gas (C.P. grade) supplied by Matheson of Canada Limited was passed slowly through liquid nitrogen traps T_1 which served to eliminate

impurities, if there were any, in the gas, and to develop pressures up to 2000 p.s.i. The gas was then compressed in the mercury-column gas compressor C and admitted into the absorption cell. After the gas reached equilibrium as indicated by the cessation of fluctuations in the intensity of radiation transmitted by the cell, absorption traces of intensity I_1 were taken until they were reproducible. A pure deuterium gas experiment consisted of obtaining absorption traces of its first overtone band at different pressures of deuterium. At the end of the experiment, the cell was re-evacuated and the background traces were taken again.

D₂-N₂ and D₂-Ar Mixture Experiments

For each mixture experiment, deuterium gas was admitted into the evacuated absorption cell with valves V_2 and V_5 closed. The base pressure of deuterium was measured by means of the gauge G_1 . Recorder traces of the intensity I_1 for a given base pressure of deuterium in the absorption cell were recorded. The valves V_1 and V_6 were then closed and the system was re-evacuated. The perturbing gas, nitrogen from a commercial cylinder or research grade argon supplied by Matheson of Canada Limited, was passed through the traps T_2 and compressed in the mercury-column gas compressor. The coolant for the traps T_2 was liquid nitrogen or liquid oxygen when nitrogen gas or argon gas was purified, respectively. The perturbing gas was then admitted into the absorption cell to the required pressures in sharp pulses by opening and closing the valves V_6 momentarily three or four times at proper intervals. The

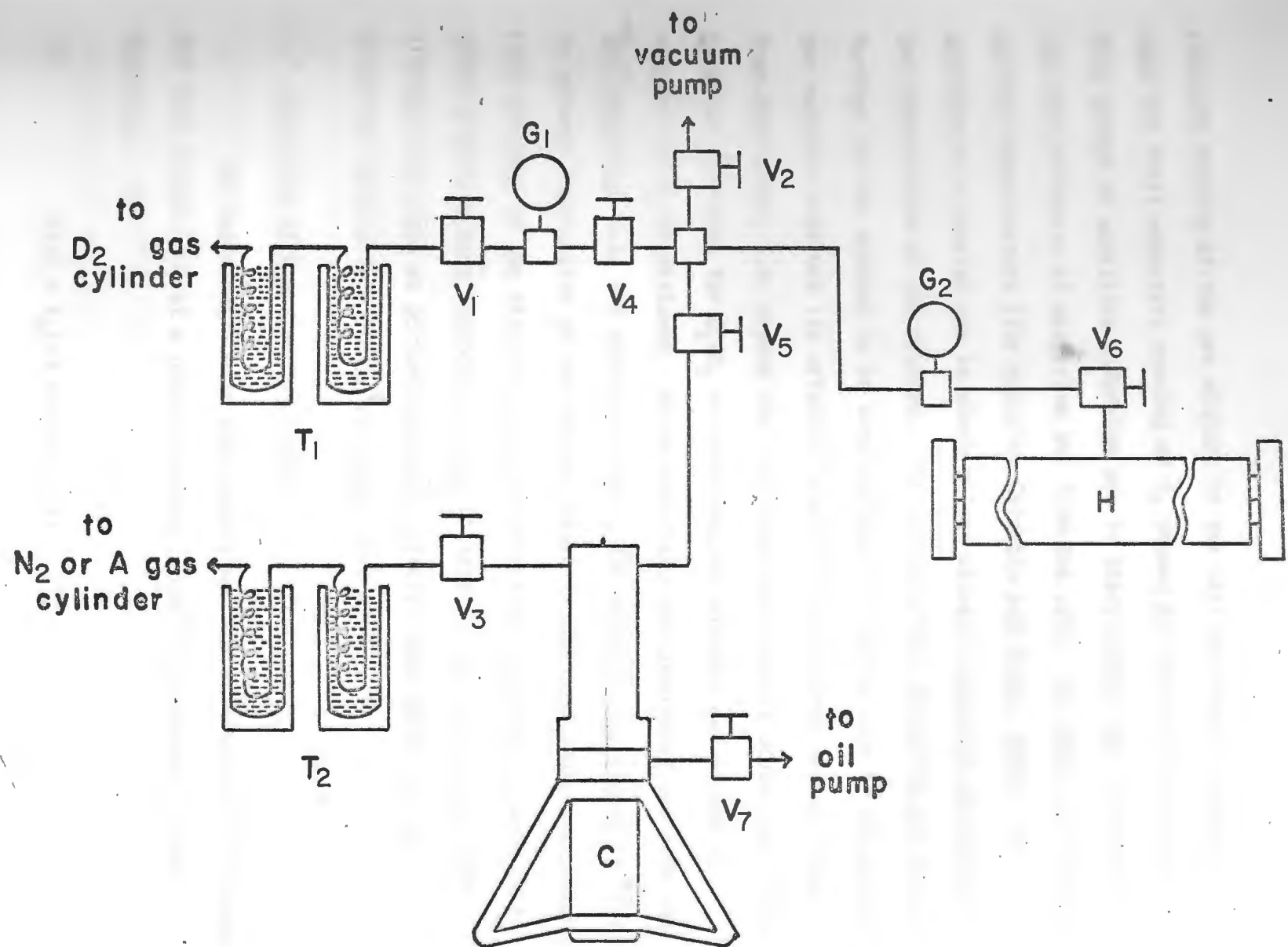


Fig. 5. The gas handling system.

pressure reading of the gas mixture in the cell was read on gauge G_2 when the final momentary opening of V_6 showed no change in pressure. This method of admitting a foreign gas in sharp pulses was to minimize the back diffusion of deuterium gas from the cell. As noted by several earlier investigators (for example, Chisholm and Welsh, 1954), the addition of a foreign gas in sharp pulses caused a peculiar variation in the transmission of the mixture. The mixing of the deuterium gas and a foreign gas was assumed to be complete when the deflection of the pen of the recorder regained its original level in the spectral region, free from absorption, i.e. beyond the first overtone band of deuterium. This duration of mixing for D_2-N_2 mixtures was 60 minutes, and it was 40 minutes for D_2-Ar mixtures. While admitting the compressed gas from the gas compressor into the absorption cell, the valve V_7 was closed in order to prevent fluctuation of the mercury level in the gas compressor. For each pressure of the mixture, recorder traces of intensity I_2 were taken until a satisfactory reproduction was obtained. For experiments with nitrogen and argon as perturbing gases, several base densities of deuterium ranging from 98 to 126 amagat were used.

2.4 Reduction of Experimental Traces

For experiments with pure deuterium, the absorption coefficient per unit length $\alpha(v)$ at a given frequency $v(cm^{-1})$ is defined by the equation,

$$(1) \quad I(v) = I_0(v) \exp \{-\alpha(v)l\}$$

where $I_0(v)$ is the intensity of radiation incident on the evacuated absorption cell of optical path ℓ in unit frequency interval at v , and $I(v)$ is the intensity transmitted by the cell containing the absorbing (pure) gas at a given density ρ_a . The enhancement in the absorption coefficient per unit path length $\alpha_{en}(v)$ due to the addition of a foreign gas at density ρ_b into the cell containing the absorbing gas at any fixed base density ρ_a is given by

$$(2) \quad I_2(v) = I_1(v) \exp \{-\alpha_{en}(v)\ell\}$$

where $I_1(v)$ is the intensity transmitted by the absorbing gas in the cell and $I_2(v)$ is the intensity transmitted by the binary gas mixture in the cell. We have, therefore, from eqs. (1) and (2),

$$(3) \quad \alpha(v) = (2.303/\ell) \log_{10} \{I_0(v)/I(v)\} ,$$

and

$$(4) \quad \alpha_{en}(v) = (2.303/\ell) \log_{10} \{I_1(v)/I_2(v)\} .$$

A standard frequency calibration chart showing the calibration peaks and a scale of wave numbers was prepared for the spectral region of the first overtone band of deuterium. The infinite absorption trace $I_\infty(v)$ was taken with a card inserted between the source and the cell. Careful frequency matching of traces was obtained using atmospheric water absorption peaks around 5300 cm^{-1} as references. The traces were then reduced by measuring $\log_{10}(I_0/I)$ for the pure gas experiments and $\log_{10}(I_1/I_2)$ for the mixture experiments at intervals of 20 cm^{-1} across the band with the help of a standard logarithmic scale. The profiles of

absorption were obtained by plotting $\log_{10}(I_0/I)$ and $\log_{10}(I_1/I_2)$ against ν . The integrated absorption coefficient $\int \alpha(\nu) d\nu$ or its enhancement $\int \alpha_{en}(\nu) d\nu$ in cm^{-2} was derived from the area under the absorption profiles.

2.5 Isothermal Data of Gases

In the study of the collision-induced spectra, the density of a gas expressed in units of amagat is used rather than its pressure because the former is more directly related to its number density (i.e. number of molecules per unit volume). Amagat is defined as the ratio of the density of a gas at a given temperature and pressure to its density at S.T.P. In the present experiments, the density of deuterium was obtained from the isothermal data given by Michels, De Graaff, Wassenaar, Levelt and Louwerse (1959). The isothermal data of nitrogen and argon were obtained from Michels and Botzen (1953) and Michels, Botzen, Friedman and Sengers (1956) respectively.

The partial densities of the component gases in a binary mixture with deuterium were determined by the following interpolation method (see Reddy and Cho (1965)). The base density of deuterium, ρ_a , was directly obtained from its isothermal data. The partial density, ρ_b , of the foreign gas was determined by using the formula

$$(5) \quad \rho_b = \{1/(1 + \beta')\} \{(\rho_a)_p + \beta'(\rho_b)_p\} - \rho_a$$

where $\beta' = \rho_b'/\rho_a$ is the approximate ratio of densities, ρ_b' being the approximate density of the foreign gas which is obtained on the assumption that the partial pressures of the component gases of the

mixture are additive. Here $(\rho_a)_p$ and $(\rho_b)_p$ are the densities of deuterium and the foreign gas, respectively, at the total pressure, P , of the mixture.

2.6 A Note on the Errors of Observation

As mentioned earlier, the first overtone band of deuterium was investigated with a slit width of 50μ . The accuracy of the frequencies of the observed peaks of the band depends upon whether the peaks are sharp or broad. In the present investigation, the spectral region was carefully calibrated with sharp emission lines from a quartz mercury lamp and with the absorption peaks of 1,2,4-trichloro-benzene and polystyrene. It was estimated that the accuracy of the frequency measurements of the observed peaks is within $\pm 3 \text{ cm}^{-1}$.

In the measurement of pressures, the 5000 p.s.i. gauge could be read with an accuracy of at least ± 20 p.s.i., which means that the fractional error for a reading of 2500 p.s.i. is $\pm 0.8\%$ while it is $\pm 0.4\%$ for a reading of 5000 p.s.i. The 20,000 p.s.i. gauge could be read with an accuracy of at least ± 70 p.s.i. which gives the fractional errors, 1.2% for a reading of 6000 p.s.i. and 0.6% for a reading of 12,000 p.s.i. The errors in the measurements of the integrated absorption coefficients may arise from errors in matching the absorption traces with the background traces. Such errors in matching can arise from the noise in the traces, the instability of the source of radiation, etc. In the present investigation, the experiments were carried out under conditions when these errors were minimum.

The derived integrated absorption coefficients (or their enhancements) of the experimental profiles depend upon the observed quantities $\log_{10}(I_0/I)$ (or $\log_{10}I_1/I_2$). The fractional errors of these integrated absorption coefficients are, in general, large or small depending on whether the total absorption to be measured is small or large, respectively. In the present investigation, the absorption to be measured for D₂-Ar profiles is relatively small compared to those for D₂-N₂ and pure D₂ profiles. The estimated fractional errors in the integrated absorption coefficients are approximately of the order of 2% to 12%.

The errors of observation in the measurement of pressures (densities) and integrated absorption coefficients are random in nature and may be in general positive or negative. In addition to these random errors, there may be a systematic error caused by the inaccuracy in establishing the infinite absorption line. The latter was minimized by checking the infinite absorption line at several intervals during an experiment.

It is rather complicated to estimate the absolute error in the values of the binary absorption coefficients obtained in the present work. However, the maximum probable errors in the values of pressures (densities) and integrated absorption coefficients given above are indicative of the maximum probable errors in the binary absorption coefficients which are derived from the plots of $(1/\rho_a^2)\int \alpha(v)dv$ or $(1/\rho_a \rho_b)\int \alpha_{en}(v)dv$ against ρ_a or ρ_b , respectively. Unless otherwise stated, the errors quoted in this thesis are standard deviations. In the derivation of the binary absorption

coefficients, the plots (see Figs. 9, 10 and 13) which are obviously straight lines were obtained using a large number of experimental points.

CHAPTER 3

EXPERIMENTAL RESULTS AND DISCUSSION

The apparatus described in the previous chapter was used to study the collision-induced 1st overtone absorption band of deuterium at room temperature (298^0K) in $\text{D}_2\text{-Ar}$ and $\text{D}_2\text{-N}_2$ mixtures and in the pure gas with an absorption path length of 194.3 cm. For argon or nitrogen as the perturbing gas, three base densities of deuterium in the range 98.2 to 125.5 amagat were used. Several partial densities of a perturbing gas were used with a given base density of deuterium. The highest partial densities reached for argon and nitrogen in amagat were 394 and 319 respectively. For the pure gas, three independent experiments were conducted for gas densities up to 455 amagat.

The profile of the induced absorption of the 1st overtone band of deuterium is dependent on the nature of the perturbing gas. In this chapter, representative sets of the experimental profiles of absorption in the pure gas and of the enhancement of absorption in $\text{D}_2\text{-Ar}$ and $\text{D}_2\text{-N}_2$ mixtures are presented, their shapes are discussed and the binary and ternary absorption coefficients are derived.

3.1 Absorption Profiles of the 1st Overtone Band of Deuterium in $\text{D}_2\text{-Ar}$, $\text{D}_2\text{-N}_2$ and Pure D_2

Typical sets of experimental profiles of the induced 1st overtone band of deuterium obtained in $\text{D}_2\text{-Ar}$ and $\text{D}_2\text{-N}_2$ mixtures and in pure D_2 at room temperature are presented in Figs. 6, 7 and 8 respectively.

For the profiles in Figs. 6 and 7, the base densities of deuterium are 101.3 amagat and 98.2 amagat respectively. The enhancements in absorption ($\log_{10} I_1/I_2$) for the mixtures and the absorption ($\log_{10} I_0/I$) for the pure gas are plotted against frequency (cm^{-1}). The positions of the single transitions (see below), $O_2(2)$, $Q_2(2)$, $S_2(J)$ ^{with} ~~for~~ $J = 0$ to 5, marked on the frequency axes, were calculated from the constants of molecular deuterium obtained by Stoicheff (1957) from the high resolution Raman spectrum of the low pressure gas and by Wilkinson (1968) from its electronic spectrum.

In the enhancement absorption profiles of D_2 -Ar mixtures (Fig. 6), the maxima of the strong quadrupolar lines $O_2(2)$, $S_2(0)$, $S_2(1)$ and $S_2(2)$ closely correspond with the calculated frequencies. Weaker quadrupolar peaks corresponding to $S_2(3)$, $S_2(4)$ and $S_2(5)$ lines are also seen. Q branch appears as a single line with a maximum at 5855 cm^{-1} . Actually at room temperature the Q branch consists of five quadrupolar lines $Q_2(J)$ with $J = 1$ to 5. In general the quadrupolar $Q_2(0)$ line does not occur because the single transition $J''(=J)=0 \rightarrow J'=0$ is forbidden. However, when the perturbing gas has a quadrupole moment, $Q_2(0)$ occurs due to double transitions. As argon is monoatomic, no double transitions occur in the enhancement absorption profiles of D_2 -Ar.

The enhancement absorption profiles of D_2 -N₂ mixtures (Fig. 7) are quite different from those of D_2 -Ar mixtures. The Q branch is very broad, the maxima of the $S_2(1)$, $S_2(2)$ and $S_2(4)$ lines are well-pronounced, and the $O_2(2)$, $S_2(0)$ and $S_2(3)$ lines appear as weak components. The Q branch consists of single transitions $Q_2(J)$ ^{with} ~~for~~ $J = 1$ to 5 and a very

Deuterium-Argon
Path length 194.3 cm
298°K

Densities
101.3 Amagat D₂
394.0 " Ar
351.0 " "
293.8 " "
221.9 " "
124.4 " "
74.3 " "

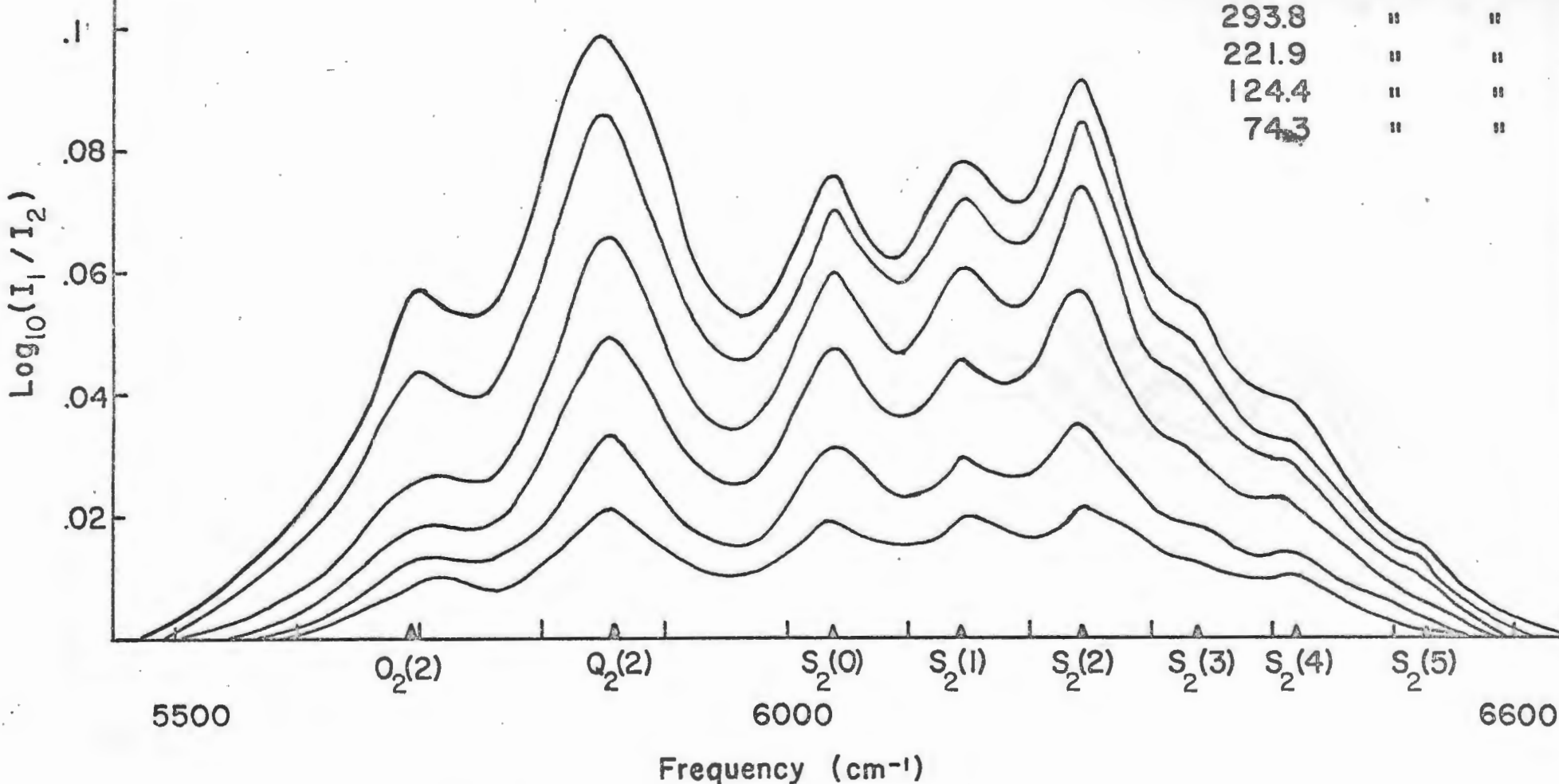


Fig. 6.. Profiles of the enhancement of absorption of the D₂ 1st overtone band in D₂-Ar mixtures.

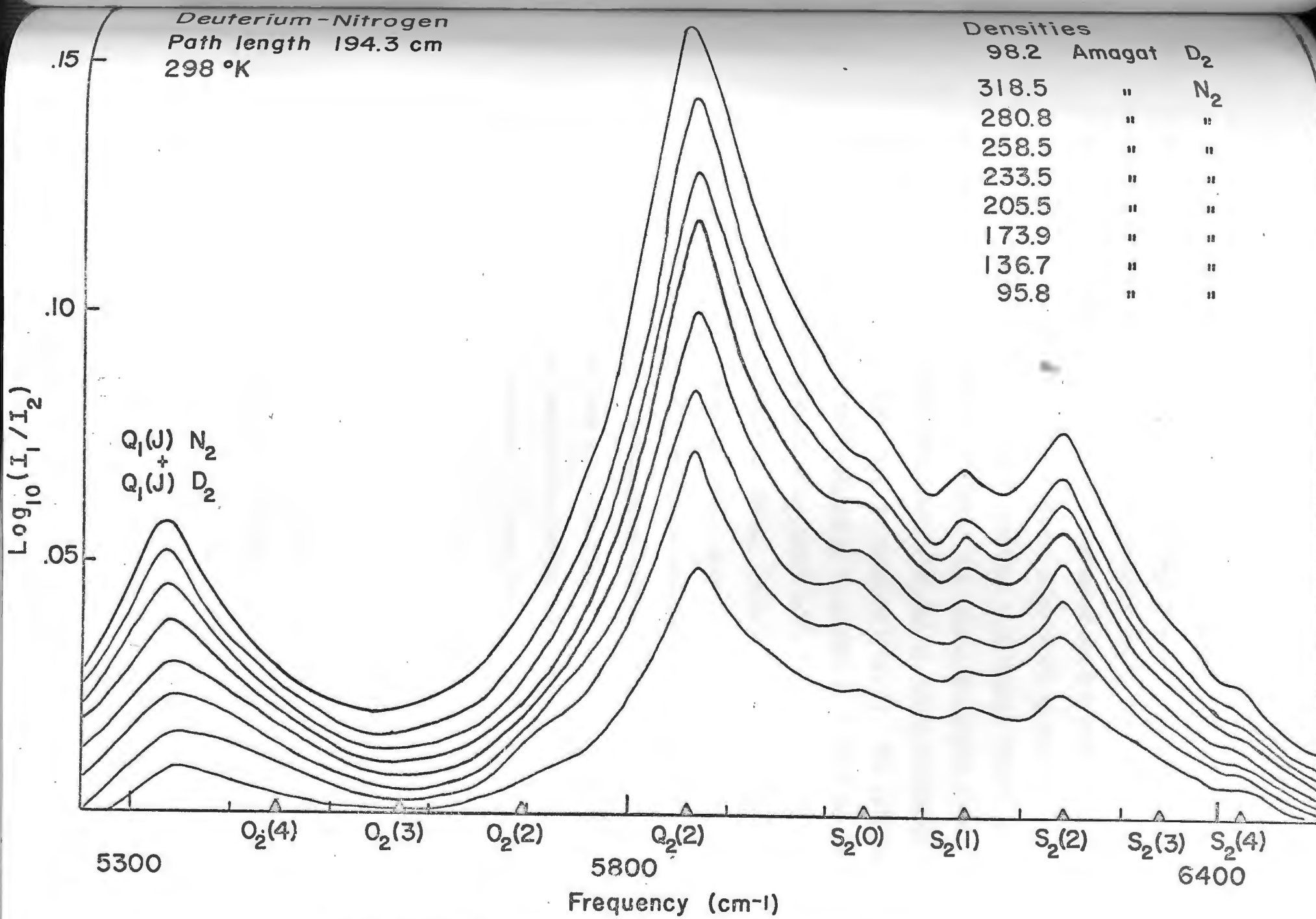


Fig. 7. Profiles of the enhancement of absorption of the
 U_2 1st overtone band in D_2-N_2 mixtures.

large number of double transitions $Q_2(J)\{D_2\} + S_0(J)\{N_2\}$. Because the rotational constant of N_2 is small ($B_0 = 1.9897 \text{ cm}^{-1}$, Stoicheff (1954)), these double transitions occur in the region of the Q branch. (In Chapter 4, the contribution of the double transitions to the total intensity of enhancement absorption profiles is estimated from an analysis of the profiles.) On the low frequency side beyond the region of the first overtone band of deuterium, absorption due to double vibrational transitions, $Q_1(J)\{D_2\} + Q_1(J)\{N_2\}$, is observed (Fig. 7). The calculated position of the origin of this absorption is at 5325 cm^{-1} which is the sum of the frequencies of $Q_1(0)$ of D_2 (2994 cm^{-1} , Stoicheff, 1957) and $Q_1(0)$ of N_2 (2331 cm^{-1} , Herzberg, 1950a). This value closely corresponds to the frequency of the observed peak. Vodar (1958) reported a similar H_2-N_2 transition in a gaseous mixture of hydrogen and nitrogen.

The features of the absorption profiles of the 1st overtone band of deuterium in the pure gas (Fig. 8) appear quite different from those of the enhancement absorption profiles obtained in D_2-Ar and D_2-N_2 mixtures. Most of the intensity of these profiles occurs in the high frequency region of the band. In the region above 5900 cm^{-1} , there are four strong but broad peaks, none of which corresponds to any of the calculated frequencies of the single transitions. However, in the low frequency region there is a slight indication of the $O_2(3)$ and $O_2(2)$ peaks. Actually the profiles of the band in the pure gas can be interpreted as a superposition of two profiles. One of these is a pure overtone profile in which (i) complete single transitions corresponding to $\Delta v=2$ and $\Delta J=0, \pm 2$ in one of the colliding molecules alone occur, and (ii) double transitions corresponding to $\Delta v=2$ and $\Delta J=0$ in one molecule

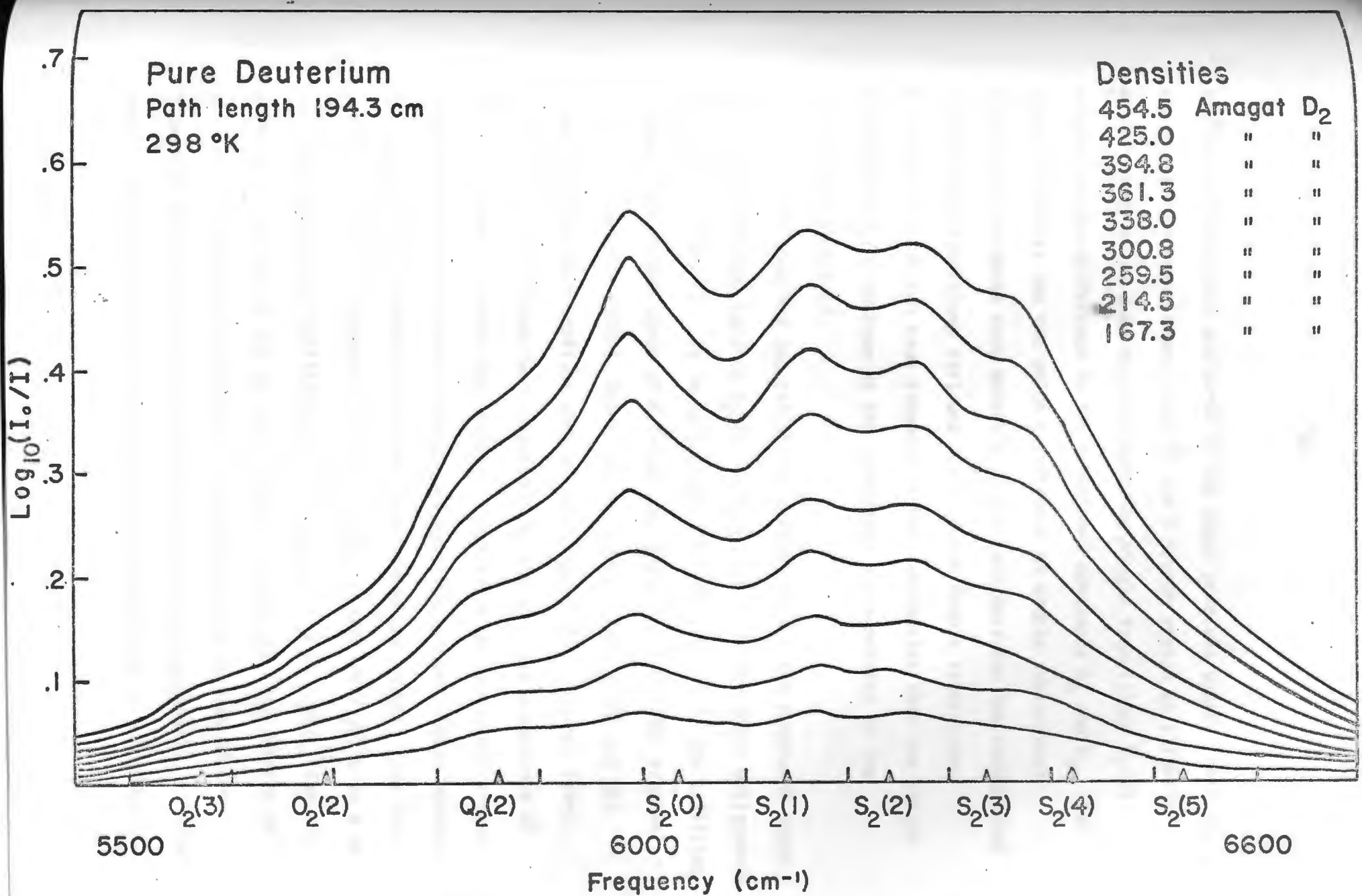


Fig. 8. Absorption profiles for the D_2 1st overtone band at

of the colliding pair and $\Delta J = \pm 2$ in the other molecule occur. Here the second type of transitions occur in the S branch region at slightly higher frequencies than the corresponding single transitions $S_2(J)$ because of the difference in the rotational constants B_0 and B_1 . The other profile is the one which corresponds to double vibrational transitions in which each molecule of the pair performs the fundamental vibrational transitions $\Delta v=1$ and $\Delta J=0$. These double transitions $Q_1(J)\{D_2\} + Q_1(J)\{D_2\}$ have somewhat higher frequencies than the single transitions $Q_2(J)$ because of the mechanical anharmonicity of the vibrational potential.

The observed and calculated frequencies of the prominent peaks of the 1st overtone band in D_2 -Ar, D_2 - N_2 and pure D_2 and their assignments are given in Table I. It is well known from the studies of the collision-induced fundamental bands of hydrogen and deuterium (see, for example, Chisholm and Welsh (1954), Reddy and Cho (1965), Pai, Reddy and Cho (1966)), that their profiles show a splitting of the Q_1 branch ($\Delta v=1$, $\Delta J=0$) into two well-resolved components Q_p and Q_R . The occurrence of the dip in the Q_1 branch was recently shown to be an inter-collisional interference effect due to correlations existing between dipole moments in successive short-range collisions (Van Kranendonk, 1968). But the profiles of the 1st overtone band of deuterium shown in Figs. 6 to 8 do not show any sign of splitting of the Q_2 branch ($\Delta v=2$, $\Delta J=0$). The absence of the dip in the Q_2 branch suggests that the contribution of the electron overlap interaction of the colliding molecules to the intensity of the induced 1st overtone bands is not appreciable; in other words, the intensity of the induced 1st overtone bands is due almost

TABLE I

Frequencies (in cm^{-1}) of absorption peaks in $\text{D}_2\text{-Ar}$, $\text{D}_2\text{-N}_2$
and $\text{D}_2\text{-D}_2$

Mixture	Assignment	Calculated frequency*	Observed frequency**
$\text{D}_2\text{-Ar}$	$\text{Q}_2(2)$	5692.2	5690
	$\text{Q}_2(3)$	5845.9	
	$\text{Q}_2(2)$	5858.5	5850
	$\text{Q}_2(1)$	5867.0	
	$\text{S}_2(0)$	6037.6	6038
	$\text{S}_2(1)$	6143.4	6144
	$\text{S}_2(2)$	6243.8	6242
	$\text{S}_2(3)$	6338.4	6340
	$\text{S}_2(4)$	6426.6	6425
	$\text{S}_2(5)$	6522.2	6520
$\text{D}_2\text{-N}_2$	$\text{Q}_1(0)\{\text{D}_2\} + \text{Q}_1(0)\{\text{N}_2\}$	5325.0	5330
	$\text{Q}_2(2)$	5858.5	5865
	$\text{Q}_2(1)$	5867.0	
	$\text{S}_2(0)$	6037.6	6040

TABLE I (Continued)

Mixture	Assignment	Calculated frequency*	Observed frequency**
D ₂ -N ₂	S ₂ (1)	6143.4	6142
	S ₂ (2)	6243.8	6245
	S ₂ (4)	6426.6	6422
D ₂ -D ₂	Q ₂ (3)	5845.9	
	Q ₂ (2)	5858.5	5845
	Q ₁ (1)	5867.0	
	Q ₁ (1)+Q ₁ (1)	5983.3	
	Q ₁ (0)+Q ₁ (1)	5985.3	5985
	Q ₁ (0)+Q ₁ (0)	5987.3	
	Q ₂ (2)+S ₀ (1)	6157.1	
	Q ₂ (1)+S ₀ (1)	6164.5	6160
	Q ₂ (0)+S ₀ (1)	6168.9	
	Q ₂ (2)+S ₀ (2)	6273.2	
	Q ₂ (1)+S ₀ (2)	6281.7	6275
	Q ₂ (0)+S ₀ (2)	6286.0	
	Q ₂ (3)+S ₀ (3)	6371.8	
	Q ₂ (2)+S ₀ (3)	6384.5	6375

*Calculated from the constants of the free molecule (Stoicheff, 1957, Wilkinson, 1968).

**Frequency accuracy is believed to be within $\pm 3 \text{ cm}^{-1}$.

entirely to the long-range quadrupolar interaction of the colliding molecules. This is confirmed from the analysis of the profiles of the 1st overtone bands of deuterium in D₂-Ar and D₂-N₂ mixtures, presented in Chapter 4 of this thesis.

3.2 Absorption Coefficients of the 1st Overtone Band of Deuterium

The enhancements of integrated absorption coefficients per unit path length, $\int \alpha_{en}(v)dv \text{ cm}^{-2}$ for the D₂-Ar and D₂-N₂ mixtures were obtained by numerical integration of the areas under the experimental profiles. For D₂-N₂ profiles, the area corresponding to the double transitions Q₁(J){D₂} + Q₁(J){N₂} is not considered. The values of these coefficients and the corresponding partial densities of deuterium and the perturbing gas argon or nitrogen for the mixture experiments are listed in Table II or Table III respectively. The enhancements of the integrated absorption coefficients show a dependence on the partial densities of deuterium and the perturbing gas which can be represented by the relation

$$(6) \quad \int \alpha_{en}(v)dv = \alpha_{1b}\rho_a\rho_b + \alpha_{2b}\rho_a\rho_b^2$$

where α_{1b} and α_{2b} are the binary and ternary absorption coefficients of the enhancement respectively. The calculated values of $(1/\rho_a\rho_b)\int \alpha_{en}(v)dv$ were plotted against ρ_b in Fig. 9 for D₂-Ar and D₂-N₂ mixture experiments. Both the plots are straight lines, the intercepts giving the binary absorption coefficients and the slopes giving the ternary absorption coefficients. The values of these coefficients obtained by a least-square fit of the experimental data are listed in Table V.

TABLE II

Enhancements of the integrated absorption coefficients of the
1st overtone band of D₂ in D₂-Ar mixtures

ρ_{D_2} (amagat)	ρ_{Ar} (amagat)	$\int \alpha_{en}(v) dv$ (cm ⁻²)	$(1/\rho_a \rho_b) \int \alpha_{en}(v) dv$ (10 ⁻⁵ cm ⁻² amagat ⁻²)
101.3*	124.4	0.22	1.71
"	176.4	0.27	1.53
"	221.9	0.34	1.50
"	260.3	0.39	1.49
"	293.8	0.44	1.48
"	328.4	0.53	1.59
"	351.0	0.56	1.59
"	372.4	0.59	1.57
"	394.0	0.66	1.65
101.3*	122.9	0.20	1.61
"	175.7	0.25	1.38
"	221.9	0.32	1.40
"	260.4	0.37	1.40
"	293.6	0.46	1.53
"	323.0	0.53	1.62

TABLE II (Continued)

ρ_{D_2} (amagat)	ρ_{Ar} * (amagat)	$\int \alpha_{en}(v) dv$ (cm ⁻²)	$(1/\rho_a \rho_b) \int \alpha_{en}(v) dv$ (10 ⁻⁵ cm ⁻² amagat ⁻²)
120.2	133.7	0.23	1.44
"	182.5	0.32	1.45
"	220.7	0.38	1.44
"	260.2	0.46	1.46
"	288.4	0.54	1.57
"	318.1	0.58	1.51
"	338.3	0.60	1.48

*Equal base densities (101.3 amagat of D₂) were used in two separate experiments.

TABLE III

Enhancements of the integrated absorption coefficients
of the 1st overtone band of D₂ in D₂-N₂ mixtures

ρ_{D_2} (amagat)	ρ_{N_2} (amagat)	$\int \alpha_{en}(\nu) d\nu$ (cm ⁻²)	$(1/\rho_a \rho_b) \int \alpha_{en}(\nu) d\nu$ (10 ⁻⁵ cm ⁻² amagat ⁻²)
98.2	95.8	0.17	1.84
"	136.7	0.27	1.98
"	173.9	0.34	2.01
"	205.5	0.41	2.02
"	233.5	0.48	2.08
"	258.5	0.55	2.17
"	280.8	0.60	2.18
"	300.4	0.68	2.31
"	318.5	0.70	2.22
101.3	106.2	0.21	2.00
"	161.8	0.31	1.87
"	187.0	0.39	2.08
"	218.1	0.45	2.05
"	245.9	0.53	2.12
"	270.8	0.58	2.10
"	292.6	0.63	2.12
"	312.3	0.66	2.10

TABLE III (Continued)

ρ_{D_2} (amagat)	ρ_{N_2} (amagat)	$\int \alpha_{en}(v) dv$ (cm $^{-2}$)	$(1/\rho_a \rho_b) \int \alpha_{en}(v) dv$ (10 $^{-5}$ cm $^{-2}$ amagat $^{-2}$)
125.5	61.7	0.14	1.76
"	104.4	0.29	2.19
"	144.6	0.39	2.12
"	188.4	0.51	2.17
"	209.1	0.60	2.29
"	235.6	0.67	2.27
"	259.6	0.76	2.34
"	278.3	0.82	2.34

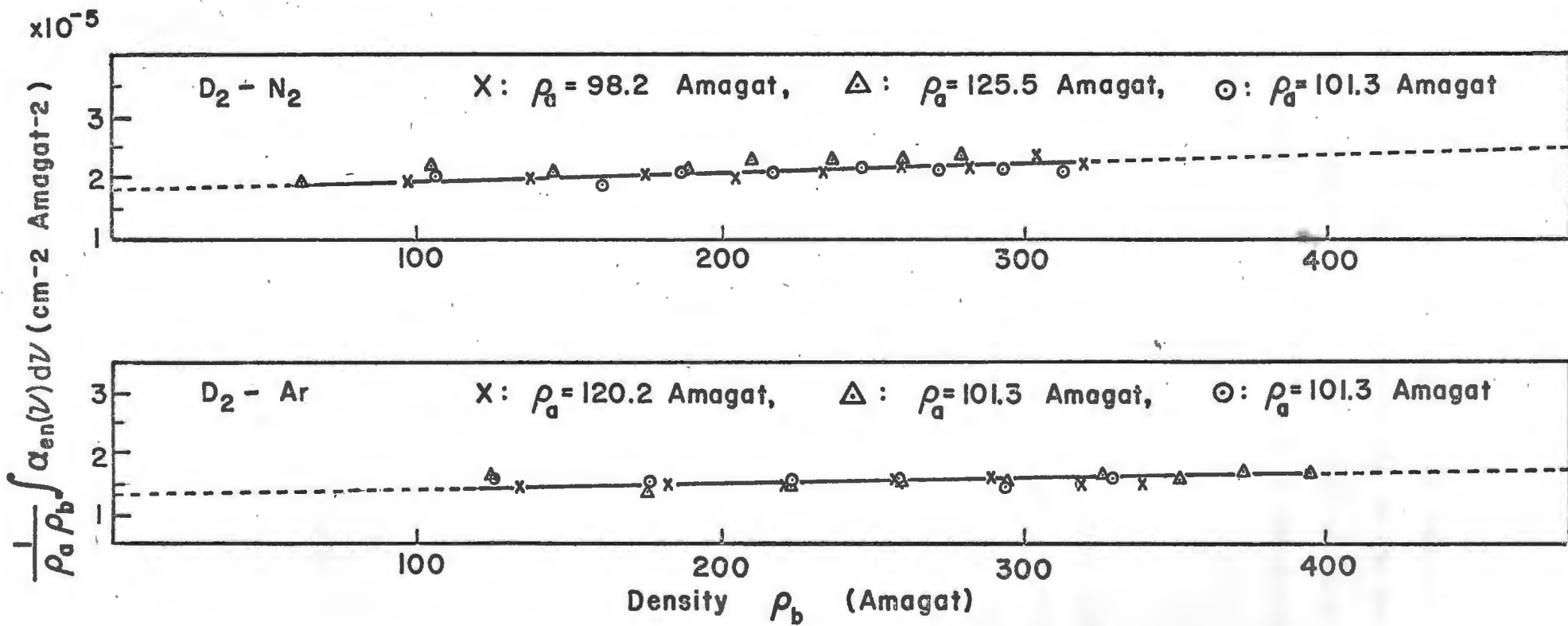


Fig. 9. Relations between the enhancements in the integrated absorption coefficients and the partial densities ρ_a and ρ_b in $D_2 - Ar$ and $D_2 - N_2$ mixtures.

For the pure gas experiments, the integrated absorption coefficients $\int \alpha(v) dv$ cm⁻² and the densities of the gas for three different independent experiments are listed in Table IV. The dependence of the integrated absorption coefficient on the density of deuterium can be represented by the relation

$$(7) \quad \int \alpha(v) dv = \alpha_{1a} \rho_a^2 + \alpha_{2a} \rho_a^3 .$$

The values of $(1/\rho_a^2) \int \alpha(v) dv$ are plotted against ρ_a in Fig. 10. The values of the binary and ternary absorption coefficients α_{1a} and α_{2a} given by the intercept and the slope respectively, obtained by a least-square fit of the experimental data, are listed in Table V. As seen from Table V, the values of the ternary absorption coefficients are small for the mixtures as well as for the pure gas.

In order to compare with the theory, the integrated absorption coefficients can be more conveniently represented as follows. For the pure gas,

$$(8) \quad c \int \tilde{\alpha}(v) dv = \tilde{\alpha}_{1a} \rho_a^2 n_0^2 + \tilde{\alpha}_{2a} \rho_a^3 n_0^3 ,$$

and for the binary mixtures,

$$(9) \quad c \int \tilde{\alpha}_{en}(v) dv = \tilde{\alpha}_{1b} \rho_a \rho_b n_0^2 + \tilde{\alpha}_{2b} \rho_a \rho_b n_0^3 ,$$

where c is the speed of light, $\tilde{\alpha}(v) = \alpha(v)/v$, and $\tilde{\alpha}_{en}(v) = \alpha_{en}(v)/v$ are the coefficients of absorption and its enhancement at a frequency v with the frequency factor removed, and $n_0 = N_A/V_0$ is Loschmidt's number (2.687×10^{19} cm⁻³). Here N_A and V_0 are the Avogadro's number and the gram-molar volume of an ideal gas at S.T.P., respectively. The new

TABLE IV

Integrated absorption coefficients of the 1st overtone band
of D₂ in the pure gas

ρ_{D_2} (amagat)	$\int \alpha(v) dv$ (cm ⁻²)	$(1/\rho_a^2) \int \alpha(v) dv$ (10 ⁻⁵ cm ⁻² amagat ⁻²)
<u>Experiment 1:</u>		
167.3	0.62	2.20
214.5	0.96	2.10
259.5	1.38	2.05
300.8	1.92	2.12
338.0	2.41	2.11
361.3	3.11	2.38
394.8	3.62	2.32
425.0	4.21	2.33
454.5	4.80	2.32
<u>Experiment 2:</u>		
122.0	0.35	2.34
173.0	0.68	2.29
238.2	1.27	2.24
267.6	1.55	2.16
312.5	2.06	2.17
340.0	2.63	2.28

TABLE IV (Continued)

ρ_{D_2} (amagat)	$\int \alpha(v) dv$ (cm ⁻²)	$(1/\rho_a^2) \alpha(v) dv$ (10^{-5} cm ⁻² amagat ⁻²)
<u>Experiment 3:</u>		
112.3	0.29	2.31
138.2	0.43	2.27
164.0	0.60	2.22
183.5	0.72	2.14
205.0	0.90	2.14
234.4	1.16	2.12

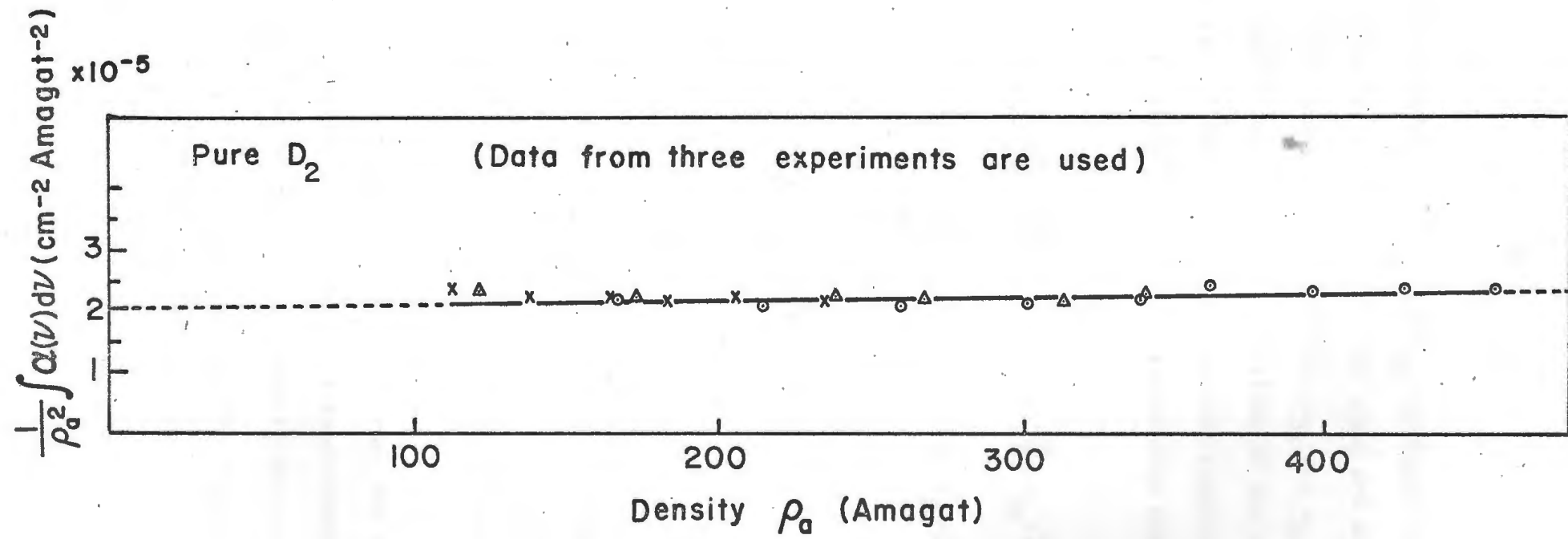


Fig. 10. Relation between the integrated absorption coefficient and the density of deuterium.

binary absorption coefficients $\tilde{\alpha}_{1a}$ and $\tilde{\alpha}_{1b}$ represent transition probabilities induced in collisions of the types a-a and a-b, respectively; and the new ternary absorption coefficients $\tilde{\alpha}_{2a}$ and $\tilde{\alpha}_{2b}$ represent the transition probabilities induced in collisions of the types a-a-a and b-a-b, respectively. The relations between the experimental absorption coefficients ($\text{cm}^{-2} \text{ amagat}^{-2}$) and the new absorption coefficients ($\text{cm}^6 \text{s}^{-1}$) are represented by

$$(10) \quad \tilde{\alpha}_{1a} = (c/n_0^2) \alpha_{1a}/\bar{v}; \quad \tilde{\alpha}_{1b} = (c/n_0^2) \alpha_{1b}/\bar{v},$$

$$\tilde{\alpha}_{2a} = (c/n_0^3) \alpha_{2a}/\bar{v}; \quad \tilde{\alpha}_{2b} = (c/n_0^3) \alpha_{2b}/\bar{v},$$

where \bar{v} , the centre of the band, is represented by

$$(11) \quad \bar{v} = \int \alpha(v) dv / \int \alpha(v) v^{-1} dv$$

or

$$\bar{v} = \int \alpha_{en}(v) dv / \int \alpha_{en}(v) v^{-1} dv.$$

The values of \bar{v} for D_2-D_2 , D_2-N_2 and D_2-Ar are 6077 cm^{-1} , 5943 cm^{-1} , 6060 cm^{-1} , respectively. The values of $\tilde{\alpha}_{1a}$ and $\tilde{\alpha}_{1b}$ in $\text{cm}^6 \text{sec}^{-1}$ for the 1st overtone band of deuterium are also included in Table V.

Finally, for the purpose of comparison, the values of the binary absorption coefficients of the collision-induced fundamental and 1st overtone bands of hydrogen and deuterium in the pure gases and their binary mixtures with nitrogen and argon at room temperature are summarized in Table VI. The ratios of the transition probabilities

TABLE V

Absorption coefficients of the induced 1st overtone band
of deuterium at 298°K*

Mixture	Binary absorption coefficient (10^{-5} cm $^{-2}$ amagat $^{-2}$)	(10^{-37} cm 6 s $^{-1}$)	Ternary absorption coefficient (cm $^{-2}$ amagat $^{-3}$)
D ₂ -D ₂	α_{1a} : 2.10 ± 0.07	$\tilde{\alpha}_{1a}$: 1.43	α_{2a} : $< 10^{-8}$
D ₂ -N ₂	α_{1b} : 1.81 ± 0.07	$\tilde{\alpha}_{1b}$: 1.26	α_{2b} : $< 10^{-7}$
D ₂ -Ar	1.30 ± 0.05	0.90	$< 10^{-8}$

*Ranges of error indicated are standard deviations.

TABLE VI

Binary absorption coefficients of the fundamental and 1st overtone bands of hydrogen and deuterium at room temperature

Mixture	Binary absorption coefficient (cm ⁻² amagat ⁻²)	(cm ⁶ s ⁻¹)	Reference
<u>Fundamental bands:</u>			
H ₂ -H ₂	2.4 x10 ⁻³	2.27x10 ⁻³⁵	Hare & Welsh (1958)
D ₂ -D ₂	1.06x10 ⁻³	1.40x10 ⁻³⁵	Reddy & Cho (1965)
H ₂ -N ₂	5.4 x10 ⁻³	5.11x10 ⁻³⁵	Hare & Welsh (1958)
D ₂ -N ₂	2.82x10 ⁻³	3.89x10 ⁻³⁵	Reddy & Varghese (unpublished, 1969)
H ₂ -Ar	4.1 x10 ⁻³	3.86x10 ⁻³⁵	Hare & Welsh (1958)
D ₂ -Ar	2.71x10 ⁻³	3.57x10 ⁻³⁵	Pai, Reddy & Cho (1966)
<u>1st overtone bands:</u>			
H ₂ -H ₂	6.2 x10 ⁻⁵		Welsh, Crawford, McDonald, Chisholm (1951)
D ₂ -D ₂	2.10x10 ⁻⁵	1.43x10 ⁻³⁷	This thesis
D ₂ -N ₂	1.81x10 ⁻⁵	1.26x10 ⁻³⁷	This thesis
D ₂ -Ar	1.30x10 ⁻⁵	0.90x10 ⁻³⁷	This thesis

(which are directly related to α_{1a} or α_{1b}) of the 1st overtone band of deuterium in pure D_2 , D_2-N_2 , and D_2-Ar to the corresponding transition probabilities of the fundamental band of deuterium are 1/98, 1/309 and 1/397, respectively.

CHAPTER 4

ANALYSIS OF THE ENHANCEMENT ABSORPTION PROFILES

4.1 Introduction

Collision-induced absorption spectra occur as a result of dipole moments induced in the molecules during collisions. One of the main characteristics of these spectra is their very broad appearance which occurs as a result of modulation of the induced dipole moment by the relative translational energy of the colliding molecules. This modulation causes a line of molecular frequency ν_m to have a frequency distribution consisting of summation and difference tones $\nu_m \pm \nu_{tr}$, where ν_{tr} is the continuum of frequencies corresponding to changes, $hc\nu_{tr}$, in the relative translational energy. At low pressures, the induced absorption is mainly due to binary collisions between molecules. At high pressures, ternary (and higher order) collisions may contribute some amount to the total absorption. At moderate pressures, the absorption profiles maintain almost constant shape although the enhancement in the integrated absorption of the band varies as the product of the densities of the absorbing and perturbing gases. In the collision-induced fundamental bands, the separation between the maxima of the overlap components Q_P and Q_R of the Q_1 branch increases with increasing density. But no splitting of the Q_2 branch of the 1st overtone band of deuterium is observed either in the pure gas or in binary mixtures of deuterium with argon or nitrogen (Chapter 3).

One must distinguish the broadening of a line in the collision-induced spectra from the ordinary pressure-broadening in the allowed spectra. Classically, individual transitions in the induced spectra give rise to very broad lines since the absorption process exists only for the duration of a collision whereas in the allowed spectra it exists unperturbed between the collisions.

In the last chapter, the frequencies of the observed peaks of the 1st overtone band of deuterium in D₂-Ar, D₂-N₂ and pure D₂ were analyzed and the binary and ternary absorption coefficients of the band were determined. In addition to these factors, the distribution of the intensity over the 1st overtone band is of interest in order to determine the parameters of a theoretical model of the induction mechanism responsible for the intensity of the band. Because of the absence of the dip in the Q branch in this band it was pointed out in the last chapter that the contribution of the short-range overlap dipole moment to the intensity of the band is negligible. This is confirmed in the present chapter by an analysis of the profiles of the band in D₂-Ar and D₂-N₂ mixtures. The details of the profile analysis and the results obtained from these are described in this chapter.

4.2 The Quadrupole-Induced 1st Overtone Band

The following three different types of molecular transitions contribute to the quadrupole-induced 1st overtone band of a symmetric diatomic molecule.

1. Single transitions:

Here molecule 1 of the colliding pair makes the transition $\Delta v_1 = 2$, $\Delta J_1 = 0, \pm 2$ ($J_1 = 0 \rightarrow J_1' = 0$), while the internal energy of molecule 2 remains unaltered. The binary absorption coefficient of the band due to single transitions is proportional to $(Q_1''\alpha_2)^2$ where Q_1'' is the second derivative of the quadrupole moment of molecule 1 with respect to its internuclear distance and α_2 is the polarizability of molecule 2. The frequencies of all the possible single transitions of the 1st overtone band of deuterium, calculated from the constants of the free molecule as determined by Stoicheff (1957) and Wilkinson (1968) are given in Table VII.

2. Double transitions (i):

Here molecule 1 makes a vibrational transition $\Delta v_1 = 2$, $\Delta J_1 = 0$, while molecule 2 makes a rotational transition $\Delta J_2 = 0, \pm 2$. For $\Delta J_2 = 0$, the spectrum consists of double-transition-quadrupolar $Q_2(J_1)$ lines which occur at the single-transition frequencies. For $\Delta J_2 = \pm 2$, the spectrum consists of double-transition lines $Q_2(J_1) \pm S_0(J_2)$ for each value of J_1 . In the pure gas, the spectrum extends to higher and lower frequencies than the single-transition spectrum because the rotational constant of the ground vibrational state is larger than that of the upper state. If molecule 2 is another symmetric diatomic molecule whose rotational constant is much smaller than that of molecule 1 (as in the case of D_2-N_2), the double transitions fall in the spectral region of the Q branch. The intensity is proportional to $(\alpha_1''Q_2)^2$ where α_1'' is the second derivative of the polarizability of molecule 1 with respect to its internuclear distance and Q_2 is the quadrupole moment of molecule 2.

TABLE VII

Calculated frequencies and relative intensities of the quadrupolar
single transitions of the 1st overtone band of D_2

Transition	Frequency (cm^{-1})	Relative intensity with respect to $S_2(2)$
$O_2(4)$	5443.9	0.1018
$O_2(3)$	5569.5	0.1166
$O_2(2)$	5692.2	0.3201
$Q_2(5)$	5812.4	0.0154
$Q_2(4)$	5829.2	0.1088
$Q_2(3)$	5845.9	0.1367
$Q_2(2)$	5858.5	0.4924
$Q_2(1)$	5867.0	0.3650
$(Q_2(0))*$	(5871.2)	0.0000
$S_2(0)$	6037.6	0.8577
$S_2(1)$	6143.4	0.6030
$S_2(2)$	6243.8	1.0000
$S_2(3)$	6338.4	0.2778
$S_2(4)$	6426.6	0.2220
$S_2(5)$	6522.2	0.0316

* $Q_2(0)$ does not occur as a single transition.

3. Double (vibrational) transitions (ii):

Here each of the colliding pair of molecules makes the vibrational transition $\Delta v = 1$, $\Delta J = 0$ giving the double-transition lines $Q_1(J_1) + Q_1(J_2)$. In the pure gas, the spectrum occurs at slightly higher frequencies than the corresponding single-transition spectrum ($Q_2(J)$). However, if molecule 2 of the colliding pair has a smaller vibrational frequency, the spectrum occurs on the low frequency side of the 1st overtone band of molecule 1. The intensity is proportional to $\{(Q_1 \alpha'_2)^2 + (\alpha'_1 Q_2)^2\}$ where the single-primed quantities are the first derivatives with respect to internuclear axes.

4.3 Relative Intensities of the Quadrupolar Single-Transition Components

The theory of the collision-induced fundamental bands of symmetric diatomic molecules has been developed by Van Kranendonk (1957, 58) using the exp-4 model for the induced dipole moment. In this model, the induced dipole moment giving rise to the absorption is expressed in terms of a short-range part ($\propto \exp(-R/\rho)$) due to the distortion of the electron charge distribution by the overlap forces, and a long-range part ($\propto 1/R^4$) due to molecular quadrupolar induction. Explicit formulae for the probabilities of the quadrupolar single and double transitions of the 1st overtone bands of symmetric molecules have been derived by Shapiro (1965) from an expression for the induced dipole moment given by Van Kranendonk (1958) in the exp-4 model.

According to the theory (see Appendix A), the relative intensities of the single-transition quadrupolar lines of the induced overtone band depend upon the following factors:

$$(12) \quad \begin{aligned} \tilde{\alpha}_{1b}\{O(J)\} &: (Q_1^{\alpha_2})^2 P(J) L_2(J, J-2) \\ \tilde{\alpha}_{1b}\{Q(J)\} &: (Q_1^{\alpha_2})^2 P(J) L_2(J, J) \\ \tilde{\alpha}_{1b}\{S(J)\} &: (Q_1^{\alpha_2})^2 P(J) L_2(J, J+2) . \end{aligned}$$

In the above expression, $P(J)$ are the normalized Boltzmann factors and $L_2(J, J')$ are the Racah coefficients. A recent theoretical calculation of Birnbaum and Poll (1969) indicates that matrix elements of the quadrupole moment between different vibrational states of deuterium $\langle vJ | Q | v+2J' \rangle$ are sensitive to the values of J and J' . In the present analysis, $Q_1^{\alpha_2}$ for different transitions are calculated from the values of the matrix elements of deuterium given by Birnbaum and Poll (1969) (also see Appendix B). The polarizability (α_2) of argon or nitrogen is considered to be a constant. The relative intensities of all the single-transition quadrupolar lines with respect to the intensity of the $S_2(2)$ line are included in Table VII.

4.4 Line Shape

As mentioned in section 4.1 above, a line of molecular frequency v_m in collision-induced spectra consists of summation and difference tones $v_m \pm v_{tr}$ (v_{tr} being the continuum of frequencies corresponding to the relative translational energy of the colliding pairs). The ratio of the populations of molecules absorbing frequencies $v_m - v_{tr}$ and $v_m + v_{tr}$ is given by the Boltzmann relation $\exp(-hc v_{tr}/kT)$. Therefore, the absorption coefficients $\tilde{\alpha}^-$ and $\tilde{\alpha}^+$ (where $\tilde{\alpha} = (1/v)\alpha$) at the frequencies $v_m - v_{tr}$ and $v_m + v_{tr}$ in the low- and high-frequency sides, respectively, should be related by the expression

$$(13) \quad \tilde{\alpha}^- = \tilde{\alpha}^+ \exp(-hc v_{tr}/kT) .$$

The profiles of the Q branch of the fundamental vibration-rotation band of hydrogen in H₂-He mixtures at 298°K and in pure hydrogen in the temperature range 18° - 77°K have been shown to satisfy the relation (13) by Chisholm and Welsh (1954) and Watanabe and Welsh (1967) respectively. The pure rotational lines of hydrogen have also been shown to obey this relation by Kiss and Welsh (1959).

The high frequency side of the quadrupolar pure rotational lines of hydrogen (Kiss and Welsh, 1959) and the high frequency side of the Q branch of the fundamental band of hydrogen (excluding the immediate region near the dip) (Hunt and Welsh, 1964) have been represented by the dispersion (or Lorentzian) form:

$$(14) \quad \tilde{\alpha}(v) = \tilde{\alpha}^0 / \{1 + (v - v_m)^2 / \delta^2\}, \quad v > v_m ,$$

where $\tilde{\alpha}^0$ is the peak absorption intensity (or a fictitious peak absorption at the band origin $v_0 (=v_m)$ of the Q branch) and δ is half of the width of line (toward high frequency side) at half intensity.

A line whose intensities in the low- and high-frequency sides are represented by eqs. (13) and (14), respectively, is said to have a Boltzmann-modified dispersion line shape. It should be noted that the pure rotational spectrum of hydrogen shows deviations from the dispersion line shape at frequencies in the region of the tail far away from the central maximum (Bosomworth and Gush, 1965, Mactaggart and Hunt, 1969). Similar deviations have been found in the Q branch of the fundamental band of hydrogen in H₂-He mixtures by Watanabe and Welsh (1967). In the

present analysis, all the quadrupolar components of the 1st overtone band of deuterium are assumed to have a simple Boltzmann-modified dispersion shape given by eqs. (13) and (14) discussed above. It will be seen that such a line shape gives a good representation of single-transition profiles of the band in D_2 -Ar and D_2 - N_2 mixtures.

4.5 Analysis of the Profiles of the 1st Overtone Band in D_2 -Ar and

D_2 - N_2 Mixtures

The analysis of the enhancement profiles of the 1st overtone band of deuterium in D_2 -Ar and D_2 - N_2 mixtures was carried out by means of a program written for the IBM 360 computer. All the single-transition quadrupolar components were assumed to have Boltzmann-modified dispersion line shapes with the same half-width δ_s . The peak intensities of these components were expressed in terms of the peak intensity of the most intense quadrupolar line $S_2(2)$ (see Table VII). No perturbation of the energy levels was assumed in the induced 1st overtone band. In the computer program, the value of the half-width was left as an adjustable parameter. The program was written such that a series of computations was carried out for different values of δ_s until the best fit of the calculated profile with the experimental profile in a desired spectral region was obtained. The criterion for the best fit was that the sum of the squares for the differences between the calculated and observed intensities at 10 cm^{-1} intervals over the desired region of the band be a minimum. When the best fit was obtained, the program enabled the computer to print out the data for the individual single-transition components of the band.

For the enhancement profiles of D_2 -Ar mixtures, the fitting was first carried out in the region $6200 - 6500 \text{ cm}^{-1}$ where S lines only contribute to the intensity of the band. When the best fit was obtained in that region, it was found that the entire region of the 1st overtone band could be fitted with no change of parameters in the program. An example of the results of the analysis for D_2 -Ar contours is shown in Fig. 11, in which $\log_{10}(I_1/I_2)(\pi/2.303)\nu\alpha_{en}(\nu)$ is plotted against the frequency. The partial densities of deuterium and argon for the profile given in Fig. 11 are 101.3 and 221.9 amagat, respectively. The 14 single-transition components of the band are shown separated out for the profile of the band. A satisfactory agreement* between the calculated and experimental profiles over the entire region of band except a slight difference in the shoulder of the Q branch indicates that the single transitions account for almost all the intensity of the band. The important conclusion which can be drawn from the analysis of the enhancement profiles of D_2 -Ar is that the contribution of the overlap forces to the intensity of the first overtone band is negligible. In contrast, it may be noted here that the overlap forces contribute as high as 75% to the total intensity of the induced fundamental band of deuterium in D_2 -Ar mixtures at room temperature (Pai, Reddy and Cho, 1966).

On the basis of the conclusion drawn above for the profiles in D_2 -Ar mixtures, it is assumed that the contribution of the overlap forces to the profiles of the band in D_2 - N_2 mixtures is negligible. Since the perturbing nitrogen gas has a quadrupole moment, double transitions $Q_2(J_1) \{D_2\} + S_0(J_2) \{N_2\}$ also contribute to the intensity

*The low frequency wing of the experimental profile (from 5400 cm^{-1} to 5600 cm^{-1}) is interfered with the water vapor absorption.

Deuterium - Argon

Path length 194.3 cm
298 °K

Densities

101.3 Amagat D_2
221.9 " Ar

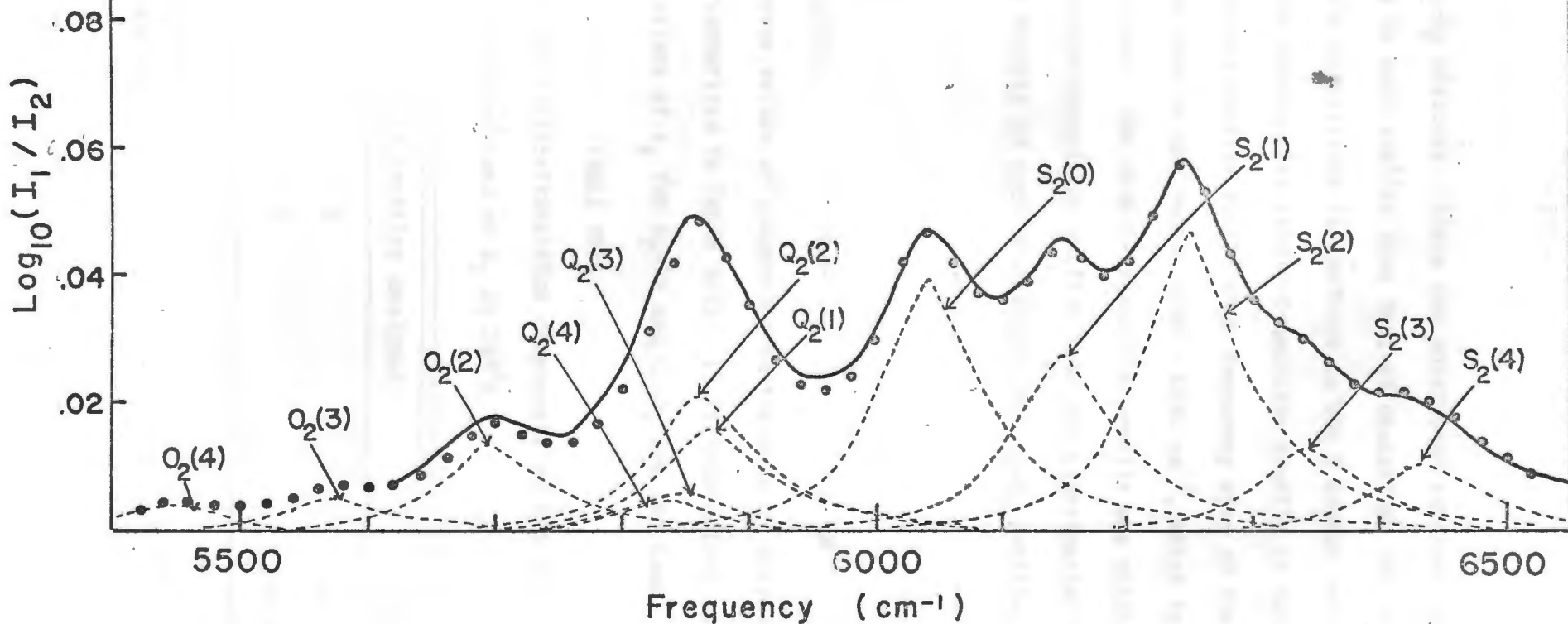


Fig. 11. Analysis of the 1st overtone band of D_2 in $D_2\text{-Ar}$ mixture. The solid curve is the experimental profile; the dashed lines indicate the individual components and the dots represent the summation of these.

of the band in D_2-N_2 mixtures. Since the rotational constant of the nitrogen molecule is much smaller than that of deuterium, the intensity due to these double transitions is confined to the Q branch region. For D_2-N_2 mixtures, the quadrupolar single-transition profile is obtained by fitting the calculated profile to the high frequency wing of the experimental profile of the band in the region $6240 - 6540 \text{ cm}^{-1}$, which is free from the double transitions. The double-transition profile was obtained by subtracting the single-transition profile from the experimental profile. An example of the results of such an analysis for D_2-N_2 profiles is shown in Fig. 12.*

4.6 Discussion

(i) Half-width:

The average values of dispersion half-widths δ_s obtained from the analysis are summarized in Table VIII. It is interesting to note that the average values of δ_s for $D_2-\text{Ar}$ and D_2-N_2 are the same.

TABLE VIII

Values of δ_s for the single-transition components of the 1st overtone band of D_2 at 298^0K

Mixture	No. of profiles analyzed	$\delta_s (\text{cm}^{-1})$
$D_2-\text{Ar}$	6	56 ± 2
D_2-N_2	8	56 ± 2

*See footnote on page 55.

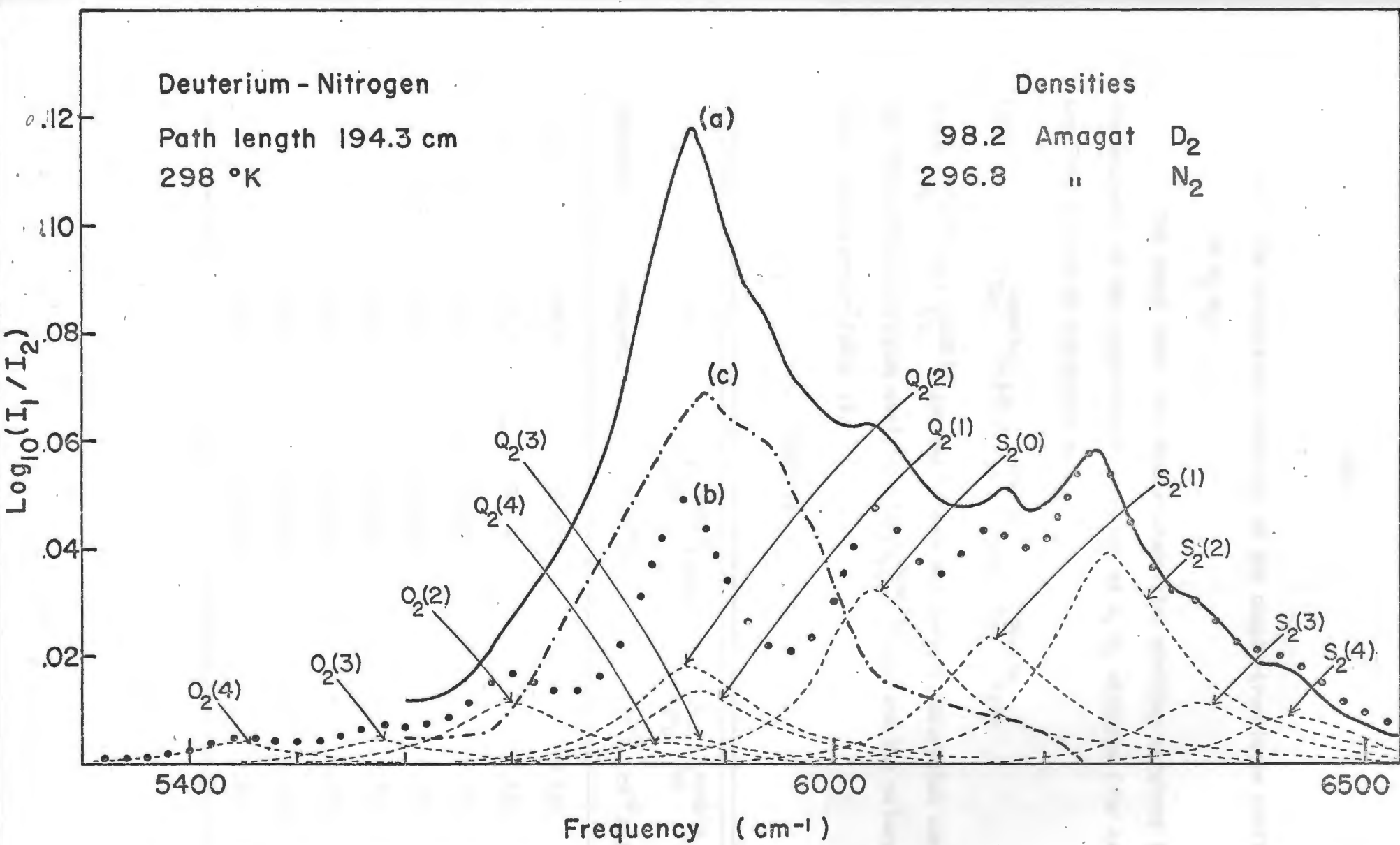


Fig. 12. Analysis of the 1st overtone band of D_2 in D_2-N_2 mixture. The dashed lines indicate the individual single transition components; (a) represents the experimental profile (b) represents the summation of the single transition components; (c) represents the profiles of the double transitions.

(ii) The integrated intensity of the double-transition profiles of D₂-N₂:

The areas under the double-transition profiles obtained from the analysis of the experimental profiles of D₂-N₂ mixtures (for example, see Fig. 12) can be expressed as

$$(15) \quad \int \alpha_{en}^{double}(v) dv = \alpha_{1b}^{double} \rho_a \rho_b + \alpha_{2b}^{double} \rho_a \rho_b^2$$

where α_{1b}^{double} and α_{2b}^{double} are the binary and ternary absorption coefficients. The integrated absorption coefficients $\int \alpha_{en}^{double}(v) dv$ and the values of ρ_a and ρ_b are given in Table IX.

TABLE IX

ρ_a (amagat)	ρ_b (amagat)	$\int \alpha_{en}^{double}(v) dv$ (cm ⁻²)	$\frac{1}{\rho_a \rho_b} \int \alpha_{en}^{double}(v) dv$ (10 ⁻⁵ cm ⁻² amagat ⁻²)
98.2	130.3	0.079	0.620
"	226.0	0.140	0.631
"	264.5	0.184	0.709
"	296.8	0.207	0.712
"	324.2	0.237	0.743
"	348.3	0.266	0.778
"	371.0	0.298	0.818
"	390.3	0.312	0.815

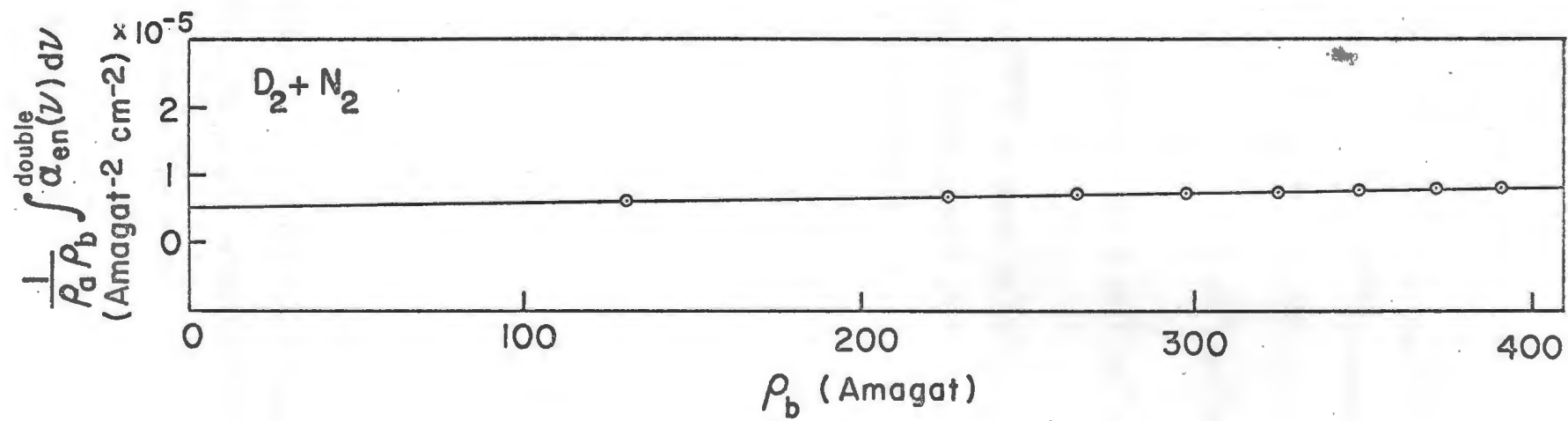


Fig. 13. Relation between the enhancements in the double-transition integrated absorption coefficients and partial densities ρ_a and ρ_b in D_2-N_2 mixtures.

The intercept and the slope of the straight line plot between $(1/\rho_a \rho_b) \int \alpha_{en}^{double}(\nu) d\nu$ against ρ_b (Fig. 13) give the values of the binary and ternary coefficients α_{1b}^{double} and α_{2b}^{double} , respectively. The values of these, obtained by a least-square fit, are

$$\alpha_{1b}^{double} = (0.48 \pm 0.03) \times 10^{-5} \text{ cm}^{-2} \text{ amagat}^{-2},$$

$$\alpha_{2b}^{double} = (0.84 \pm 0.10) \times 10^{-7} \text{ cm}^{-2} \text{ amagat}^{-3}.$$

The binary coefficient $\tilde{\alpha}_{1b}^{double}$ in units of $\text{cm}^6 \text{s}^{-1}$ is 0.34×10^{-37} ($\tilde{\alpha}_{1b}^{double} = (c/n_0^2) \alpha_{1b}^{double} / \bar{\nu}$, $\bar{\nu}$ being 5900 cm^{-1}). The binary absorption coefficient due to single transitions, $\tilde{\alpha}_{1b}^{single}$ ($= \alpha_{1b} - \alpha_{1b}^{double}$) is $1.33 \times 10^{-5} \text{ cm}^{-2} \text{ amagat}^{-2}$. The corresponding value of $\tilde{\alpha}_{1b}^{single}$ is $0.90 \times 10^{-37} \text{ cm}^6 \text{s}^{-1}$ (here $\bar{\nu}$ being 6060 cm^{-1}).

(iii) Evaluation of the quadrupole moment of the nitrogen molecule

The ratio of the binary absorption coefficients of the double to single transitions of the 1st overtone band of D_2 in D_2-N_2 mixtures can be expressed as

$$(16) \quad \frac{\tilde{\alpha}_{1b}^{double}}{\tilde{\alpha}_{1b}^{single}} = \left[\frac{\alpha_1'' Q_2}{Q_1'' \alpha_2} \right]^2$$

where α_1 and Q_1 are respectively the quadrupole moment and polarizability of the deuterium molecule, the double prime indicates the second derivative with respect to the internuclear distance of the molecule, and Q_2 and α_2 are respectively the quadrupole moment and the polarizability of the nitrogen molecule. The value of α_1'' obtained from the matrix

element of the polarizability $\langle v | \alpha | v+2 \rangle$ (Poll, private communication, 1970) is 1.735 a_0 . The value of Q_1'' obtained from the matrix element $\langle v | Q | v+2 \rangle$ (Birnbaum and Poll, 1969) is $-0.272e$. The polarizability of the nitrogen molecule, α_2 , is 11.936 a_0^3 (Bridge and Buckingham, 1964). The value of the quadrupole moment of nitrogen, Q_2 , as calculated from eq. (16), is $1.14 \pm 0.05 \text{ ea}_0^2$. This value is in good agreement with the value 1.1 ea_0^2 obtained previously by Poll (1963), and Reddy and Cho (1965a). The reasonable value obtained for the quadrupole moment of nitrogen in the present work implies that the assumption, namely the contribution of the overlap forces to the intensity of the band in D_2-N_2 mixtures is negligible, is valid.

APPENDIX A

THE THEORY OF COLLISION-INDUCED INFRARED ABSORPTION

In this appendix we first review briefly the theory of the collision-induced infrared absorption of the fundamental bands of symmetric diatomic molecules and then give an account of the theory of the induced absorption of the 1st overtone bands of these molecules. We follow this procedure because the form of the expressions for the long-range quadrupolar induction responsible for the 1st overtone infrared absorption is similar to that for the long-range induction for the fundamental infrared absorption.

Fundamental band:

The binary absorption coefficient of a definite rotational branch of the 1 \leftrightarrow 0 vibrational band is expressed as

$$(A-1) \quad \alpha_1(B) = \kappa \sum^{(B)} P_1 P_2 |M_1(\omega_1 \omega_2; R_{12})|^2 g_0(R_{12}) dR_{12}$$

by Van Kranendonk (1957, 58). Here the suffixes 1 and 2 denote the colliding molecules, $\kappa = \pi/3m_0 v_0$, m_0 being the reduced mass of the absorbing molecule, v_0 being the frequency of the band origin, P_1 and P_2 are the normalized Boltzmann factors for the initial states of molecules 1 and 2, respectively, R_{12} is the line joining the centres of the mass of the two colliding molecules, and $g_0(R_{12})$ is the pair distribution function. The quantity $M_1 (\equiv \langle (\frac{\partial M}{\partial r})_0 \rangle)$ can be expanded as (Van Kranendonk, 1958)

$$(A-2) \quad M_1(\omega_1 \omega_2; R_{12}) = 4\pi \sum_{\lambda_1 \mu_1 \lambda_2 \mu_2} D(\lambda_1 \mu_1 \lambda_2 \mu_2; R_{12}) Y_{\lambda_1}^{\mu_1}(\omega_1) Y_{\lambda_2}^{\mu_2}(\omega_2)$$

where $\omega_1 = (\theta_1, \phi_1)$ and $\omega_2 = (\theta_2, \phi_2)$ are the polar angles of the inter-nuclear axes of the molecules 1 and 2, relative to a coordinate frame XYZ in which the vector R_{12} lies along the Z-axis, μ_1 and μ_2 are the quantum numbers of the projection, along an axis perpendicular to R_{12} , of the momenta Λ_1 (of quantum number λ_1) and Λ_2 (of quantum number λ_2), and $Y_{\lambda}^{\mu}(\omega)$ are the spherical harmonic functions (see Appendix D). The expansion coefficients D have the components D_{μ} in the same coordinate frame which are characteristic of the pair of colliding molecules. For the possible values 1, 0, -1 for μ , their coefficients are given by

$$(A-3) \quad D_{\pm 1} = \frac{1}{\sqrt{2}} (D_x \pm i D_y); \quad D_0 = D_z .$$

For homonuclear diatomic molecules, there is no permanent dipole moment, the coefficients D_{μ} are then different from zero only for even values of λ_1 and λ_2 . In the exp-4 model for the induced electronic dipole moment, components D_{μ} of (A-3) are assumed to have the following values:

$$(A-4) \quad D_0(0000) = \xi \exp(-R/\rho) ,$$

$$D_0(2000) = (3/\sqrt{5}) Q_1^1 \alpha_2^1 / R^4 : \text{single transitions}$$

$$D_{\pm 1}(2\pm 100) = (3/\sqrt{15}) Q_1^1 \alpha_2^1 / R^4 : " "$$

$$D_0(0020) = -(3/\sqrt{5}) \alpha_1^1 Q_2^1 / R^4 : \text{double transitions}$$

$$D_{\pm 1}(002\pm 1) = -(3/\sqrt{15}) \alpha_1^1 Q_2^1 / R^4 : " "$$

Here $Q_1' = (\frac{\partial Q_1}{\partial r_1})_0$ and $\alpha_1' = (\frac{\partial \alpha_1}{\partial r_1})_0$, r_1 being the internuclear distance in molecule 1; Q_1 and α_1 are the quadrupolar moment and average polarizability of molecule 1, respectively, while Q_2 and α_2 are the corresponding quantities of molecule 2.

Substituting (A-2) into (A-1), the resulting expression for the binary absorption coefficient of a definite rotational branch B can be written in the form:

$$(A-5) \quad \tilde{\alpha}_1(B) = \kappa \sum_{\lambda_1 \lambda_2} L_{\lambda_1 \lambda_2}(B) I_0(\lambda_1 \lambda_2)$$

where

$$(A-6) \quad L_{\lambda_1 \lambda_2}(B) = \sum^{(B)} P(J_1)P(J_2)L_{\lambda_1}(J_1, J'_1)L_{\lambda_2}(J_2, J'_2)$$

and

$$(A-7) \quad I_0(\lambda_1 \lambda_2) = \int \sum_{\mu_1 \mu_2} |D(\lambda_1 \mu_1 \lambda_2 \mu_2; R_{12})|^2 g_0(R_{12}) dR_{12},$$

$\sum^{(B)}$ is a sum over all the rotational quantum numbers J_1, J_2, J'_1, J'_2 for which the rotational transitions $(J_1 J_2 \rightarrow J'_1 J'_2)$ contribute to the branch B, and $P(J)$ (see Appendix C) is the Boltzmann factor for the rotational states normalized in such a way that

$$(A-8) \quad \sum_J (2J+1)P(J) = 1$$

and $L(J, J')$ are the Racah coefficients (see Appendix D) defined by

$$(A-9) \quad \begin{aligned} & \frac{1}{4\pi} \sum_{mm'} \langle J m | \lambda \mu J' m' \rangle \langle \lambda' \mu' J' m' | J m \rangle \\ & = L_{\lambda \lambda'}(J, J') \delta_{\lambda \lambda'} \delta_{\mu \mu'}, \end{aligned}$$

which must satisfy the condition

$$(A-10) \quad \sum_J \sum_{J'} L_\lambda(J, J') P(J) = 1$$

where

$$\sum_J \sum_{J'} L_\lambda(J, J') = 2J + 1 .$$

But

$$\langle J_m | \lambda \mu J' m' \rangle = \int Y_J^{m*}(\omega) Y_\lambda^\mu(\omega) Y_{J'}^{m'}(\omega) d\omega .$$

Substitution of (A-4) into (A-7) gives the non-vanishing integrals,

$$(A-11) \quad \langle I_0(00) = \lambda^2 \mathbf{J} \tilde{\gamma} ;$$

$$\langle I_0(20) = \mu_1^2 \mathbf{J} \tilde{\gamma} ;$$

$$\langle I_0(02) = \mu_2^2 \mathbf{J} \tilde{\gamma} .$$

The dimensionless parameters λ , μ_1 and μ_2 are defined as

$$(A-12) \quad \lambda = (\varepsilon/e) e^{-\sigma/\rho}; \quad \mu_1 = Q_1 \alpha_2 \epsilon^4 ;$$

$$\mu_2 = \alpha_1 Q_2 \epsilon^4 ;$$

where σ is the intermolecular distance R for which the intermolecular potential is zero, and e is the absolute value of the electronic charge.

The significance of λ is that λe is the amplitude of the oscillating overlap dipole moment when the molecules are a distance σ apart, and $\mu_1 e$ and $\mu_2 e$ have similar meanings, $\tilde{\gamma}$ is defined by

$$(A-13) \quad \tilde{\gamma} = \frac{\pi e^2 \sigma^3}{3m_0 v_0}$$

where m_0 and ν_0 are the reduced mass and the frequency of oscillation (in s^{-1}), respectively, of the absorbing molecule (1). The quantities of \mathbf{I} and \mathbf{J} are the dimensionless radial distribution integrals defined by

$$(A-14) \quad \mathbf{I} = 4\pi \int_0^{\infty} \exp(-2(x-1)\frac{\sigma}{\rho}) g_0(x) x^2 dx$$

and

$$(A-15) \quad \mathbf{J} = 12\pi \int_0^{\infty} x^{-8} g_0(x) x^2 dx$$

where $x = R/\sigma$ and $g_0(x)$ is the low density limit of the pair distribution function expressed as $g_0(x) = \exp(-V(x)/kT)$. Here $V(x)$ is taken as the Lennard-Jones intermolecular potential ($V(x) = 4\epsilon(x^{-12} - x^{-6})$).

On substituting (A-11), the expression (A-5) becomes

$$(A-16) \quad \tilde{\alpha}_1(B) = \{\lambda^2 \mathbf{I} L_{00}(B) + \mu_1^2 \mathbf{J} L_{20}(B) + \mu_2^2 \mathbf{J} L_{02}(B)\} \tilde{\gamma} .$$

Finally, using the relations (A-6), (A-10) and (A-16), the binary absorption coefficient $\tilde{\alpha}_1 (\equiv \sum^{(B)} \tilde{\alpha}_1(B))$ of the total 1 + 0 can be written as

$$(A-17) \quad \tilde{\alpha}_1 = \lambda^2 \mathbf{I} \tilde{\gamma} + (\mu_1^2 + \mu_2^2) \mathbf{J} \tilde{\gamma} .$$

Here the first term $\lambda^2 \mathbf{I} \tilde{\gamma}$ represents the contribution due to the short-range overlap electron induction and the remaining term represents the contribution due to the long-range quadrupolar induction.

The 1st overtone band:

In general the matrix element R^{nm} of the induced dipole moment in a binary collision between molecules 1 and 2 can be represented as

$$(A-18) \quad R^{nm} = \int \psi_n^* M \psi_m d\tau \\ = \langle v_1' v_2' J_1' J_2' | M | v_1' v_2' J_1' J_2' \rangle .$$

For the fundamental band

$$(A-19) \quad R^{nm} = \langle 0 0 J_1 J_2 | M_1 | 1 0 J_1' J_2' \rangle$$

where R^{nm} is the matrix element of the dipole moment corresponding to all possible single and double transitions. The corresponding matrix element for the 1st overtone band is

$$(A-20) \quad R^{nm} = \langle 0 0 J_1 J_2 | M_2 | 2 0 J_1' J_2' \rangle \\ + \langle 0 0 J_1 J_2 | M_2 | 1 1 J_1' J_2' \rangle .$$

For the pure gas, the second term in the above expression corresponds to vibrational transitions in which each of the colliding molecules makes one fundamental transition. However, for mixtures (example, D_2-N_2), the second term gives rise to an absorption band at a frequency different from the band arising from the first term because of the difference in the vibrational frequencies of the colliding molecules. If the induced dipole moment due to quadrupolar induction is expanded as a Taylor's series in terms of the internuclear distances r_1 and r_2 and the vibrational and rotational wave functions of molecule 1 are separated, the matrix element can be written approximately as

$$(A-21) \quad R^{nm} = \frac{1}{2} \langle 0 | (r_1 - r_0)^2 | 2 \rangle \langle 0 J_1 | \frac{\partial^2 M}{\partial r_1^2} | 0 J_1 \rangle$$

$$\begin{aligned}
 &= \frac{1}{2} \langle 0 | (r_1 - r_0)^2 | 2 \rangle \langle (\frac{\partial^2 M}{\partial r_1^2})_0 \rangle \\
 &= \frac{1}{\sqrt{2}} k_1^2 \langle (\frac{\partial^2 M}{\partial r_1^2})_0 \rangle \\
 &= \frac{k_1}{\sqrt{2}} k_1 \langle (\frac{\partial^2 M}{\partial r_1^2})_0 \rangle
 \end{aligned}$$

where $k_1 = (h/8\pi^2 m_0 v_0)^{1/2}$, m_0 and v_0 being the reduced mass and frequency (s^{-1}), respectively, of molecule 1. In this expression, the matrix element corresponds to all single transitions in molecule 1 and double transitions in which molecule 1 makes the vibrational transition only and molecule 2 makes the rotational transition only. On comparing the expression (A-21) with the one for the fundamental band, $R^{nm} = k_1 \langle (\frac{\partial M}{\partial r_1})_0 \rangle$, we see that R^{nm} for the 1st overtone band contains an extra factor of $k_1/\sqrt{2}$. We now define the expansion coefficients $E(\lambda_1^{\mu_1} \lambda_2^{\mu_2}; R_{12})$ for $\langle (\frac{\partial M}{\partial r_1^2})_0 \rangle (= M_2(\omega_1 \omega_2; R_{12}))$ of the 1st overtone band, in analogy to the theory of the fundamental band (also see Shapiro, 1965) by

$$(A-22) \quad M_2(\omega_1 \omega_2; R_{12}) = 4\pi \sum_{\lambda_1^{\mu_1} \lambda_2^{\mu_2}} E(\lambda_1^{\mu_1} \lambda_2^{\mu_2}; R_{12}) Y_{\lambda_1}^{\mu_1}(\omega_1) Y_{\lambda_2}^{\mu_2}(\omega_2)$$

where the coefficients are assumed to have the following form

$$(A-23) \quad E_0(2000) = +(3/\sqrt{5})(k_1/\sqrt{2}) Q_1^{\alpha_2} R^{-4} : \text{single transitions}$$

$$E_{\pm}(2\pm 100) = +(3/\sqrt{15})(k_1/\sqrt{2}) Q_1^{\alpha_2} R^{-4} : " "$$

$$E_0(0020) = -(3/\sqrt{5})(k_1/\sqrt{2}) Q_1^{\alpha_2} R^{-4} : \text{double transitions}$$

$$E_{\pm 1}(002\pm 1) = -(3/\sqrt{15})(k_1/\sqrt{2}) Q_1^{\alpha_2} R^{-4} : " "$$

where Q_1 and α_1 are the quadrupolar moment and polarizability of molecule 1, respectively, and Q_2 and α_2 are the corresponding quantities of molecule 2. Here the double prime represents the second derivative with respect to the internuclear axis. In analogy to (A-16) of the fundamental band, the binary absorption coefficient due to the quadrupolar induction alone for the 1st overtone band can be written as

$$(A-24) \quad \tilde{\alpha}_1(B) = (k_1^2/2) \left\{ \left(\frac{Q_1 \alpha_2}{e\sigma} \right)^2 L_{20}(B) + \left(\frac{\alpha_1 Q_2}{e\sigma} \right)^2 L_{02}(B) \right\} \mathbf{J} \cdot \tilde{\gamma} .$$

If $\frac{Q_1 \alpha_2}{e\sigma} = \theta_1$ (say), and $\frac{\alpha_1 Q_2}{e\sigma} = \theta_2$ (say), the induced transitions of the O, Q and S branches for the 1st overtone band of the pure gas are given by

$$(A-25) \quad \tilde{\alpha}_{1a}\{O(J)\} = (k_1^2/2) \{ \theta_1^2 + \theta_2^2 \} \cdot P(J) \cdot L_2(J, J-2) \cdot \mathbf{J} \cdot \tilde{\gamma}$$

$$\tilde{\alpha}_{1a}\{Q(J)\} = (k_1^2/2) \{ \theta_1^2 \cdot P(J) \cdot L_2(J, J) + \theta_2^2 \cdot P(J)$$

$$\cdot L_0(J, J) \cdot P(J') \cdot L_2(J', J') \} \cdot \mathbf{J} \cdot \tilde{\gamma}$$

$$\tilde{\alpha}_{1a}\{S(J)\} = (k_1^2/2) \{ \theta_1^2 + \theta_2^2 \} \cdot P(J) \cdot L_2(J, J+2) \cdot \mathbf{J} \cdot \tilde{\gamma}$$

and for a binary mixture, we have the expressions

$$(A-26) \quad \tilde{\alpha}_{1b}\{O(J)\} = (k_1^2/2) \theta_1^2 \cdot P(J) \cdot L_2(J, J-2) \cdot \mathbf{J} \cdot \tilde{\gamma}$$

$$\tilde{\alpha}_{1b}\{Q(J)\} = (k_1^2/2) \{ \theta_1^2 \cdot P(J) \cdot L_2(J, J) + \theta_2^2 \cdot P(J) \cdot L_0(J, J) \} \cdot \mathbf{J} \cdot \tilde{\gamma}$$

$$\tilde{\alpha}_{1b}\{S(J)\} = (k_1^2/2) \theta_1^2 \cdot P(J) \cdot L_2(J, J+2) \cdot \mathbf{J} \cdot \tilde{\gamma} .$$

By adding the three equations in (A-25) or in (A-26) after summation over J , the binary absorption coefficient for the 1st overtone band can be represented as

$$(A-27) \quad \ddot{\alpha}_{1a} \text{ or } \ddot{\alpha}_{1b} = (k_1^2/2) \{ \theta_1^2 + \theta_2^2 \} \mathbf{J} \tilde{\gamma} .$$

For the double vibrational transitions,

$$(A-28) \quad R^{nm} = < 0 | (r_1 - r_0) | 1 > < 0 | r_2 - r_0 | 1 > < (\frac{\partial^2 M}{\partial r_1 \partial r_2})_0 >$$

$$= k_1^2 < (\frac{\partial^2 M}{\partial r_1 \partial r_2})_0 > \quad \text{for the pure gas,}$$

$$= k_1 k_2 < (\frac{\partial^2 M}{\partial r_1 \partial r_2})_0 > \quad \text{for the mixtures.}$$

(In the mixtures, k_1 and k_2 are different; for example, for the double vibrational band of D_2-N_2 .) For the case of the pure gas, factor k_1 again appears in the expansion coefficients. Again, in analogy to the theory of the fundamental band, the expansion coefficients $F(\lambda_1 \mu_1 \lambda_2 \mu_2; R_{12})$ for $< (\partial^2 M / \partial r_1 \partial r_2)_0 > (\equiv M_{12}(\omega_1 \omega_2; R_{12}))$ can be written in the following way

$$(A-29) \quad M_{12}(\omega_1 \omega_2; R_{12}) = 4\pi \sum_{\lambda_1 \mu_1 \lambda_2 \mu_2} F(\lambda_1 \mu_1 \lambda_2 \mu_2; R_{12}) Y_{\lambda_1}^{\mu_1}(\omega_1) Y_{\lambda_2}^{\mu_2}(\omega_2)$$

where

$$(A-30) \quad F_0(2000) = +(3/\sqrt{5}) k_1 Q_1^1 \alpha_2^1 R^{-4}$$

$$F_{\pm 1}(2\pm 100) = +(3/\sqrt{15}) k_1 Q_1^1 \alpha_2^1 R^{-4}$$

$$F_0(0020) = -(3/\sqrt{5}) k_1 \alpha_1^1 Q_2^1 R^{-4}$$

$$F_{\pm 1}(002\pm 1) = -(3/\sqrt{15}) k_1 \alpha_1^1 \alpha_2^1 R^{-4} .$$

The binary absorption coefficient for the double-vibration-transition band is

$$(A-31) \quad \tilde{\alpha}_1^{\text{double}} = k_1^2 \left\{ \left(\frac{Q_1 \alpha_1}{e\sigma} \right)^2 + \left(\frac{\alpha_1 Q_2}{e\sigma} \right)^2 \right\} J \tilde{\gamma}$$
$$= k_1^2 (\phi_1^2 + \phi_2^2) J \tilde{\gamma} .$$

APPENDIX B

MATRIX ELEMENTS OF THE QUADRUPOLE MOMENT FOR THE TRANSITIONS IN THE 1ST OVERTONE BAND OF DEUTERIUM

The quadrupole moment of a molecule like H_2 for the fixed nuclei, referred to a coordinate system with the Z-axis along the internuclear axis of the molecule, is given in units of ea_0^2 by

$$(B-1) \quad Q(r) = \frac{1}{2}r^2 - \langle 3Z_1^2 - r_1^2 \rangle$$

where r is the internuclear distance of the molecule and Z_1 and r_1 are the Z-coordinate and radius vector of one of the electrons in the ground electronic state. The matrix elements of the quadrupole moment, referred to the fixed frame of the molecule, between two normalized states of nuclear motion ψ_{vJ} and $\psi_{v'J'}$ of the ground electronic state are

$$(B-2) \quad \langle v J | Q | v' J' \rangle = \int \psi_{vJ}^*(r) Q(r) \psi_{v'J'}(r) dr .$$

The adiabatic values of the matrix elements in (B-2) have been evaluated recently for the more intense transitions of the Q and S branches of the 1-0, 2-0, 3-0, 4-0 and 5-0 bands of H_2 , HD and D_2 by Karl and Poll (1967) and Birnbaum and Poll (1969). These authors have determined the functions $\psi_{vJ}(r)$ in (B-2) in the adiabatic approximation (i.e. by using the adiabatic potential for the ground electronic state neglecting the influence of the excited electronic states) by solving the Schrödinger equation numerically

$$(B-3) \quad \frac{d^2\psi_{vJ}}{dr^2} + \left[\frac{4\pi\mu c}{\hbar} \{E - U(r)\} - \frac{J(J+1)}{r^2} \right] \psi_{vJ} = 0 .$$

In this expression, the above authors have used the values of the effective potential $U(R)$ of H_2 from the work of Kolos and Wolniewicz (1964, 1965, 1968). Also in (B-2), they have used the values of $Q(r)$ of H_2 from the work of Kolos and Wolniewicz (1965). It must be noted here that the function $Q(r)$ is approximately the same for isotopic molecules H_2 , HD and D_2 , but the differences between their corresponding matrix elements of the quadrupolar moment $\langle v J | Q | v' J' \rangle$ are due to their differences in their nuclear masses.

In order to calculate the relative strengths of the quadrupolar lines of the 1st overtone band of D_2 at room temperature, the values of the matrix elements $\langle 0 J | Q | 2 J' \rangle$ for $J = 0$ to 5 in the Q and S branches and $J = 2$ to 5 in the O branch are required. Birnbaum and Poll (1969) have given the values of the matrix elements for $J = 0, 1, 2$ only in the Q and S branches. We describe below the method of calculation of the matrix elements of the remaining lines of the 1st overtone band of D_2 .

Karl and Poll (1967) expanded the radial wave functions ψ_{vJ} with $J \neq 0$ in terms of the "unperturbed" functions ψ_{v0} . They represented the correction, $\Delta Q \langle v J | v' J' \rangle$, to the matrix elements due to rotation-vibration interaction by the relation

$$(B-4) \quad \langle v J | Q | v' J' \rangle = \langle v 0 | Q | v' 0 \rangle + \Delta Q \langle v J | v' J' \rangle .$$

From the first order perturbation theory

$$\Delta Q \langle v J | v' J' \rangle = - v_1^{\Sigma} \sum_{v' \neq v} \frac{\langle v' 0 | Q | v_1 0 \rangle \langle v_1 0 | v | v 0 \rangle}{E_{v_1 0} - E_{v 0}}$$

$$- v_2^{\Sigma} \neq v' \frac{\langle v \ 0 \ | \ Q \ | \ v_2 \ 0 \rangle \langle v_2 \ 0 \ | \ v' \ | \ v' \ 0 \rangle}{E_{v_2 0} - E_{v' 0}}$$

Here the perturbations \neq and v' are given by

$$v = J(J+1) \hbar^2 / 2\mu r^2, \quad v' = J'(J'+1) \hbar^2 / 2\mu r^2.$$

For approximate calculations of the matrix elements, the wave functions ψ_{v0} are approximated by harmonic oscillator wave functions. This procedure is justified whenever the matrix elements of $Q(r)$ and r^{-2} in the harmonic oscillator approximation are close to the actual values (for example, when $\Delta v = 0$ and $\Delta v = 1$). When Δv is large, the contribution of anharmonic terms to the matrix elements is no longer negligible. However, in the present calculations, harmonic-oscillator approximation is assumed to be valid for the case of the 1st overtone band of D_2 . For the purpose of this approximate calculation, $Q(r)$ and $V(r)$ are now expanded in terms of $(r - r_e)$ up to the second order.

$$Q(r) = Q_0 + Q_1(r - r_e) + Q_2(r - r_e)^2$$

$$V(r) = BJ(J+1) \left[1 - \{2(r - r_e)/r_e\} + \{3(r - r_e)^2/r_e^2\} \right]$$

where $B = \hbar^2 / 2\mu r_e^2$, r_e is internuclear distance at equilibrium position.

The relevant matrix elements in the harmonic-oscillator approximation are

$$\langle v \ | \ Q \ | \ v \rangle = Q_0 + Q_2 r_e^2 (B/\omega) (2v + 1)$$

$$\langle v \ | \ Q \ | \ v+1 \rangle = Q_1 r_e (B/\omega)^{1/2} (v + 1)^{1/2}$$

$$\langle v | Q | v+2 \rangle = Q_2 r_e^2 (B/\omega) (v+1)^{1/2} (v+2)^{1/2}$$

and

$$\langle v | V | v+1 \rangle = -2BJ(J+1)(B/\omega)^{1/2} (v+1)^{1/2}$$

$$\langle v | V | v+2 \rangle = 3BJ(J+1)(B/\omega)(v+1)^{1/2} (v+2)^{1/2} .$$

The constants Q_0 , Q_1 and Q_2 are obtained by means of a polynomial fit of $Q(r)$ versus r using the data for H_2 from the work of Kolos and Wolniewicz (1965). From (B-4), we have

$$\begin{aligned}
 (B-5) \quad \Delta Q \langle 0 J | 2 J' \rangle &= -v_1^{\sum \neq v} \frac{\langle 2 0 | Q | v_1 0 \rangle \langle v_1 0 | V | 0 0 \rangle}{E_{v_1 0} - E_{00}} \\
 &\quad - v_2^{\sum \neq v} \frac{\langle 0 0 | Q | v_2 0 \rangle \langle v_2 0 | V | 2 0 \rangle}{E_{v_2 0} - E_{20}} \\
 &\approx -\frac{\langle 2 0 | Q | 1 0 \rangle \langle 1 0 | V | 0 0 \rangle}{E_{10} - E_{00}} \\
 &\quad - \frac{\langle 2 0 | Q | 2 0 \rangle \langle 2 0 | V | 0 0 \rangle}{E_{20} - E_{00}} \\
 &\quad - \frac{\langle 0 0 | Q | 0 0 \rangle \langle 0 0 | V | 2 0 \rangle}{E_{00} - E_{20}} \\
 &\quad - \frac{\langle 0 0 | Q | 1 0 \rangle \langle 1 0 | V | 2 0 \rangle}{E_{10} - E_{20}} \\
 &= 2\sqrt{2}Q_1 r_e (B/\omega)^2 \{J(J+1) - J'(J'+1)\}
 \end{aligned}$$

$$- \frac{3\sqrt{2}}{2} Q_0 (B/\omega)^2 \{J(J+1) - J'(J'+1)\}$$

$$- \frac{3\sqrt{2}}{2} Q_2 r_e^2 (B/\omega)^3 \{5J(J+1) - J'(J'+1)\} .$$

For the D_2 molecule, $B_0 = 30.459 \text{ cm}^{-1}$, $\omega = 2993.548 \text{ cm}^{-1}$, $r_e = 0.74143 \text{ \AA} = 1.4010 \text{ a}_0$ (Stoicheff, 1957). The matrix elements $\langle 0 J | Q | 2 J' \rangle$ for the Q, S and O branches of the 1st overtone band of deuterium obtained with the use of (B-4) and (B-5) are listed in Table B-1. The values obtained by Birnbaum and Poll (1969) are also listed in the same table.

TABLE B-1

J	Q branch		S branch	O branch
	$\langle 0 J Q 2 J \rangle$	$\langle 0 J Q 2 J+2 \rangle$	$\langle 0 J+2 Q 2 J \rangle$	
0	- 0.00767*		- 0.00794*	
1	- 0.00769*		- 0.00808*	
2	- 0.00771*		- 0.00818*	- 0.00743
3	- 0.00773		- 0.00825	- 0.00727
4	- 0.00775		- 0.00837	- 0.00715
5	- 0.00777		- 0.00850	- 0.00709

*Values listed by Birnbaum & Poll (1969).

APPENDIX C

NORMALIZED BOLTZMANN FACTORS OF THE ROTATIONAL LEVELS OF THE GROUND VIBRATIONAL STATE OF D₂

In thermal equilibrium, the number of molecules N_J in any rotational state J of a symmetric diatomic gas depends on the following three factors:

(i) the Boltzmann distribution:

$$\exp(-E_J/kT) \propto \exp(-B_0 J(J+1)hc/kT) ,$$

(ii) the (2J+1)-fold degeneracy (g_J),

(iii) the degeneracy (g_T) due to nuclear spin.

The last factor for molecular deuterium is calculated as follows. The nuclear spin I of a deuterium atom is 1. The nuclear spin T of a deuterium molecule has 2I+1 values: 2(parallel spins), 1(inclined spins) and 0(antiparallel spins). Even and odd T values are possible for symmetric and antisymmetric rotational levels, respectively. For D₂ whose ground electronic state is a ¹Σ_g⁺, the even rotational levels (J = 0, 2, 4, ...) are symmetric and the odd rotational levels (J = 1, 3, 5, ...) are antisymmetric. The statistical weights 2T+1 for the even and odd J levels of D₂ are 6 {5 (for T = 2) + 1 (for T = 0)} and 3 (for T = 1), respectively. The total number of molecules N are given by

$$(C-1) \quad N = \sum_J N_J$$

$$\propto \sum_{T,J} g_T g_J \exp(-B_0 J(J+1)hc/kT)$$

$$\propto \left\{ \sum_{\text{even } J} 6(2J+1) \exp(-B_0 J(J+1)hc/kT) + \sum_{\text{odd } J} 3(2J+1) \exp(-B_0 J(J+1)hc/kT) \right\} .$$

We shall now define the normalized Boltzmann factor $P(J)$ for an initial rotational state J such that the following normalization condition is satisfied:

$$(C-2) \quad \sum_J (2J+1) P(J) = 1 .$$

$P(J)$ is then represented by

$$(C-3) \quad P(J) = \frac{g_T \exp(-B_0 J(J+1)hc/kT)}{\sum_{T,J} g_T g_J \exp(-B_0 J(J+1)hc/kT)} .$$

One must realize that the above normalization condition is valid if the Racah coefficients are used in the calculation of relative strengths of the individual lines in a band. However, if the Clebsch-Gordan coefficients are used, $P(J)$ is normalized in a different way. Then $P(J)$ has an additional factor g_J in the numerator of expression (C-3).

The calculated values of $P(J)$ for deuterium gas at room temperature (298^0K) are listed in the following table. (Note:
 B_0 of $\text{D}_2 = 30.459 \text{ cm}^{-1}$.)

TABLE C-1

J	g_J	g_T	$\exp\left(\frac{-B_0 J(J+1)hc}{kT}\right)$	relative N_J	P(J)	$(2J+1)P(J)$
0	1	6	1.000	6.000	0.1823	0.1823
1	3	3	0.7507	6.756	0.0684	0.2052
2	5	6	0.4230	12.690	0.0771	0.3855
3	7	3	0.1789	3.757	0.0163	0.1141
4	9	6	0.0568	3.068	0.0111	0.0999
5	11	3	0.0135	0.446	0.0012	0.0132
6	13	6	0.0024	0.187	0.0004	0.0052
7	15	3	0.0003	0.015	0.0000 ₃	0.0005

$$\sum_J (2J + 1)P(J) = 1.0059 \approx 1$$

APPENDIX D

RACAH COEFFICIENTS OF DIFFERENT BRANCHES IN THE INDUCED VIBRATION-ROTATION SPECTRA

The induced infrared absorption bands consist of the three branches Q, Q and S corresponding to the selection rule $\Delta J = -2, 0$ and 2 . The Racah coefficients $L_\lambda(J, J')$ are defined by (see for example, Van Kranendonk, 1958)

$$(D-1) \quad L_\lambda(J, J') \delta_{\lambda\lambda'} \delta_{mm'} = 4\pi \sum_{mm'} \int Y_J^{m*}(\omega) Y_\lambda^{\mu}(\omega) Y_{J'}^{m'}(\omega) d\omega \\ \cdot \int Y_J^m(\omega) Y_{\lambda'}^{\mu*}(\omega) Y_{J'}^{m*}(\omega) d\omega \\ = 4\pi \sum_{mm'} \int Y_J^{m*}(\omega) Y_\lambda^{\mu}(\omega) Y_{J'}^{m'}(\omega) d\omega \{ \int Y_J^{m*}(\omega) Y_{\lambda'}^{\mu*}(\omega) Y_{J'}^{m*}(\omega) \}^* .$$

Rose (1957) showed that

$$(D-2) \quad \int Y_{J_3 m_3}^* Y_{J_2 m_2} Y_{J_1 m_1} d\omega = \left[\frac{(2J_1+1)(2J_2+1)}{4\pi(2J_3+1)} \right]^{\frac{1}{2}} C(J_1 J_2 J_3) \\ m_1 m_2 m_3 \cdot C(J_1 J_2 J_3, 0 0 0)$$

where the first Clebsch-Gordan coefficient C contains the angular momenta selection rule and the second coefficient C contains the parity selection rule. Therefore

$$(D-3) \quad L_\lambda(J, J') = 4\pi \sum_{mm'} \left[\frac{(2J'+1)(2\lambda+1)}{4\pi(2J+1)} \right]^{\frac{1}{2}} C(J' \lambda J, m' \mu m)$$

$$\begin{aligned}
 & \cdot C(J' \lambda J, 000) \cdot \left[\frac{(2J'+1)(2\lambda+1)}{4\pi(2J+1)} \right]^{\frac{1}{2}} \\
 & \cdot C(J' \lambda J, m' \mu m)^* C(J' \lambda J, 000)^* \\
 & = \sum_{mm'} \frac{(2J'+1)(2\lambda+1)}{(2J+1)} C(J' \lambda J, m' \mu m)^2 C(J' \lambda J, 000)^2.
 \end{aligned}$$

Using the symmetry relation of Clebsch-Gordan coefficients,

$$C(J_1 J_2 J_3, m_1 m_2 m_3) = (-1)^{J_1-m_1} \left[\frac{2J_3+1}{2J_2+1} \right]^{\frac{1}{2}} C(J_1 J_3 J_2, m_1-m_3-m_2)$$

we have

$$\begin{aligned}
 (D-4) \quad L_\lambda(J, J') &= \sum_{mm'} (2J'+1) C(J' J \lambda, m'-m-\mu)^2 C(J' \lambda J, 000)^2 \\
 &= (2J'+1) C(J' \lambda J, 000)^2 \\
 &= (2J+1) C(J \lambda J', 000)^2 .
 \end{aligned}$$

Condon and Shortley (1953) showed that when $\lambda = 2$, the Clebsch-Gordan coefficients for the O, Q and S branches are given respectively by

$$(D = 5) \quad C(J 2 J-2, 000) = \sqrt{\frac{3}{2} \frac{J(J-1)}{(2J-1)(2J+1)}} ,$$

$$C(J 2 J, 000) = \frac{-J(J+1)}{\sqrt{(2J-1)(2J+3)J(J+1)}} ,$$

$$C(J 2 J+2, 000) = \sqrt{\frac{3}{2} \frac{(J+1)(J+2)}{(2J+1)(2J+3)}} .$$

When we substitute these relations in (D-4), the resulting Racah coefficients are

$$(D-6) \quad L_2(J, J-2) = \frac{3}{2} \frac{J(J-1)}{(2J-1)},$$

$$L_2(J, J) = \frac{J(J+1)(2J+1)}{(2J-1)(2J+3)},$$

$$L_2(J, J+2) = \frac{3}{2} \frac{(J+1)(J+2)}{(2J+3)}.$$

The values of the Racah coefficients for different transitions corresponding to the initial rotational states $J = 0$ to 5 are listed in Table D-1.

TABLE D-1

J	O Branch: $L_2(J, J-2)$	Q Branch: $L_2(J, J)$	S Branch: $L_2(J, J+2)$
0		0.000	1.000
1		1.200	1.800
2	1.000	1.429	2.571
3	1.800	1.867	3.333
4	2.571	2.338	4.091
5	3.333	2.821	4.846

ACKNOWLEDGMENTS

The author wishes to express his gratitude to his supervisor, Dr. S. P. Reddy for his invaluable guidance and encouragement during the course of the work and in the preparation of this thesis.

The author is grateful to Dr. G. Varghese for helpful discussions. He is also grateful to Professors S. W. Breckon and C. W. Cho for their interest in this investigation.

Thanks are gratefully extended to Mr. S. N. Ghosh for his assistance in the computer programming. Thanks are due to Mr. J. Tucker and Mr. P. Robinson of the Technical Services of Memorial University of Newfoundland who constructed the 2m high-pressure absorption cell. The cooperation of Mr. T. White and Mr. R. Tucker during the experiments and the preparation of some diagrams is appreciated. The use of facilities of the computer centre is acknowledged.

The award of a fellowship of Memorial University of Newfoundland and the financial support received from Dr. Reddy's N. R. C. grant (A. 2440) are gratefully acknowledged.

REFERENCES

- Birnbaum, A. and Poll, J. D. (Preprint of a paper, 1969).
- Bosomworth, D. R. and Gush, H. P. Can. J. Phys. 43, 751 (1965).
- Bridge, N. J. and Buckingham, A. D. J. Chem. Phys. 40, 2733 (1964).
- Chisholm, B. A. and Welsh, H. L. Can. J. Phys. 32, 291 (1954).
- Condon, E. U. and Shortley, G. H. The Theory of Atomic Spectra, Cambridge Univ. Press, London (1953).
- Hare, W. F. J. and Welsh, H. L. Can. J. Phys. 36, 88 (1958).
- Herzberg, G. Can. J. Res. A, 28, 144 (1950).
- Herzberg, G. Spectra of Diatomic Molecules (D. Van Nostrand Company, Inc., Princeton, New Jersey, U.S.A.).
New Jersey, New York, 1950a).
- Humphreys, C. J. J. Opt. Soc. Am. 43, 1027 (1953).
- Hunt, J. L. Ph.D. Thesis, University of Toronto (1959).
- Hunt, J. L. and Welsh, H. L. Can. J. Phys. 42, 873 (1964).
- Karl, G. and Poll, J. D. J. Chem. Phys. 46, 2944 (1967).
- Kiss, Z. J. and Welsh, H. L. Can. J. Phys. 37, 1249 (1959).
- Kolos, W. and Wolniewicz, L. J. Chem. Phys. 41, 3663 (1964).
- Kolos, W. and Wolniewicz, L. J. Chem. Phys. 43, 2429 (1965).
- Kolos, W. and Wolniewicz, L. J. Chem. Phys. 49, 404 (1968).
- Mactaggart, J. W. and Hunt, J. L. Can. J. Phys. 47, 51 (1969).
- Michels, A., De Graaff, W., Wassenaar, T., Levelt, J. M. H. and Louwerse, P. Physica, 25, 25 (1959).
- Michels, A. and Botzen, A. Physica, 19, 585 (1953).
- Michels, A., Botzen, A., Friedman, A. S. and Sengers, J. V. Physica, 22, 121 (1956).

- Pai, S. T., Reddy, S. P. and Cho, C. W. Can. J. Phys. 44, 2893 (1966).
- Plyler, E. K., Blaine, L. K. and Nowak, M. J. Res. Natl. Bur. Stds. 58, 195 (1957).
- Poll, J. D. (Private Communication, 1970).
- Poll, J. D. Phys. Letters, 7, 32 (1963).
- Reddy, S. P. and Cho, C. W. Can. J. Phys. 43, 793 (1965).
- Reddy, S. P. and Cho, C. W. Can. J. Phys. 43, 2331 (1965a)
- Reddy, S. P. and Varghese, G. (to be published).
- Rose, M. E. Elementary Theory of Angular Momentum, J. Wiley and Sons, New York (1957).
- Russell, W. E. M.Sc. Thesis, Memorial University of Newfoundland (1968).
- Shapiro, M. M. Ph.D. Thesis, University of Toronto (1965).
- Sinha, B. B. M.Sc. Thesis, Memorial University of Newfoundland (1967).
- Stoicheff, B. P. Can. J. Phys. 32, 630 (1954).
- Stoicheff, B. P. Can. J. Phys. 35, 730 (1957).
- Varghese, G. and Reddy, S. P. Can. J. Phys. 47, 2745 (1969).
- Van Kranendonk, J. Physica, 23, 825 (1957).
- Van Kranendonk, J. Physica, 24, 347 (1958).
- Van Kranendonk, J. Can. J. Phys. 46, 1173 (1968).
- Vodar, B. Proc. Conf. Mol. Spectry., MacMillan (Pergamon), New York (1958).
- Watanabe, A. Ph.D. Thesis, University of Toronto (1964).
- Watanabe, A. and Welsh, H. L. Can. J. Phys. 43, 818 (1965).
- Watanabe, A. and Welsh, H. L. Can. J. Phys. 45, 2857 (1967).
- Welsh, H. L., Crawford, M. F. and Locke, J. L. Phys. Rev. 75, 850 (1949).
- Welsh, H. L., Crawford, M. F., MacDonald, R. E. and Chisholm, D. A. Phys. Rev. 83, 1264 (1951).
- Wilkinson, P. G. Can. J. Phys. 46, 1225 (1968).

